Electrochemical Society

UNIV. OF MICHIGAN
SEP 11 1953
EAST ENGINEERING
LIBRARY

ELECTROCHEMICAL INDUSTRY

Southern California-Nevada Area

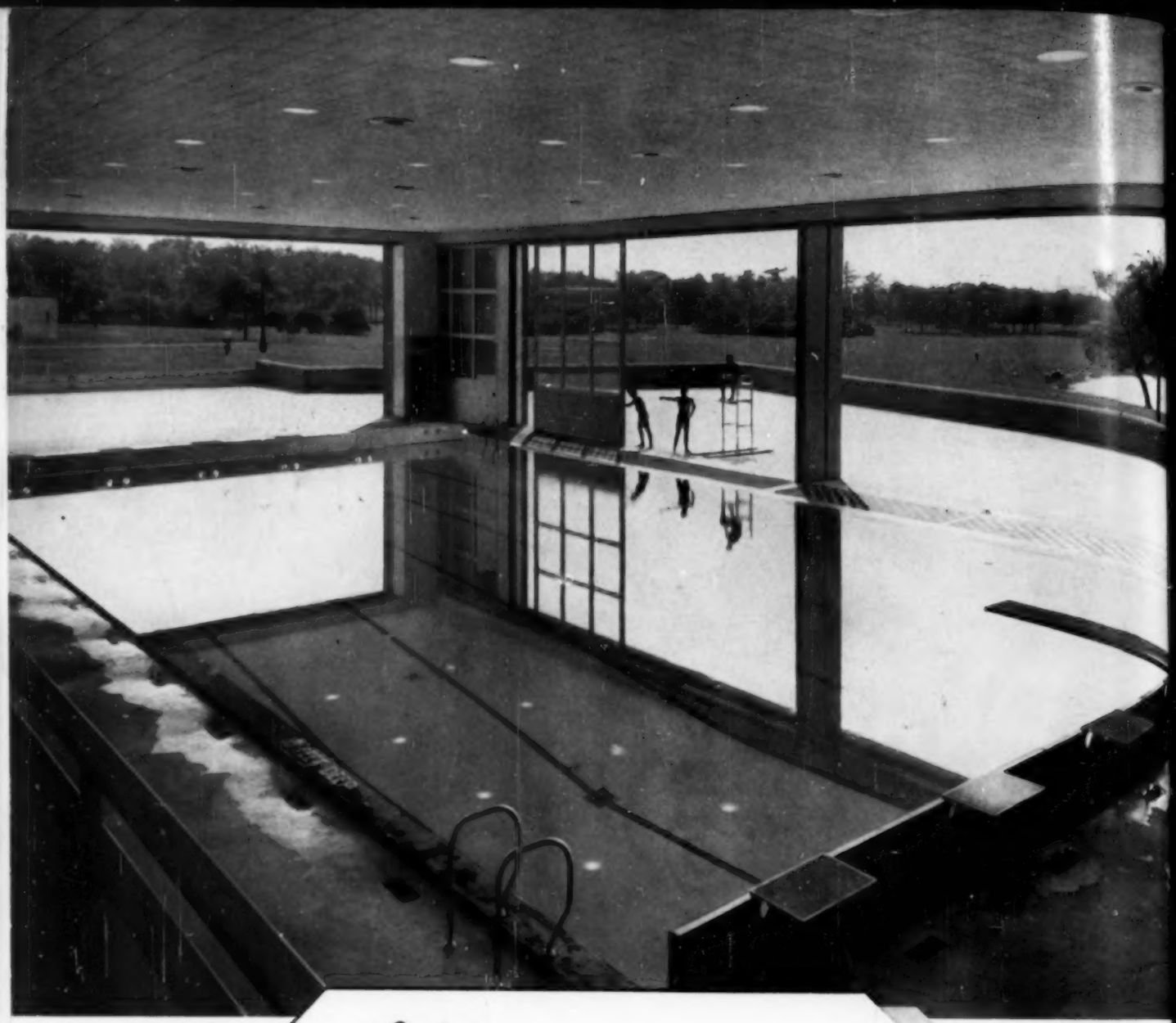

Pool in General George S. Patton Memorial Community Building, Detroit

Photo courtesy Giffels & Valle... L. Rossetti, Associated Engine... and Architects, Detroit

Chlorine ...

for water purification

Wherever water purification is needed, chlorine does the job safely, effectively, economically.

Uniformly high quality GLC Graphite Anodes are on the job too—helping the electrolytic industry meet the growing civilian and defense needs for chlorine and caustic soda.

ELECTRODE DIVISION

Great Lakes Carbon Corporation

Niagara Falls, N. Y. GLC Morganton, N. C.

Graphite Anodes, Electrodes, Molds and Specialties

Sales office: Niagara Falls, N. Y. **Other offices:** New York, N. Y., Chicago, Ill., Pittsburgh, Pa...

Sales Agents: J. B. Hayes, Birmingham, Ala., George O'Hara, Long Beach, Cal., Great Northern Carbon & Chemical Co., Ltd., Montreal, Can...

EDITORIAL STAFF

R. M. Burns, *Chairman*

Norman Hackerman, *Technical Editor*

Ruth G. Sterns, *Managing Editor*

Cecil V. King, *Associate Editor*

J. B. Thomas, *News Editor*

Mary F. Murray, *Assistant Editor*

DIVISIONAL EDITORS

J. V. Petrocelli, *Corrosion*

Abner Brenner, *Electrodeposition*

W. C. Vosburgh, *Battery*

H. C. Froelich, *Electronics*

W. C. Gardiner, *Industrial Electrolytic*

S. J. Sindeband, *Electrothermic*

John J. Chapman, *Electric Insulation*

L. B. Rogers, *Theoretical*

Sherlock Swann, Jr., *Electro-Organic*

REGIONAL EDITORS

Joseph Schulein, *Pacific Northwest*

J. C. Schumacher, *Los Angeles*

O. W. Storey, *Chicago*

G. W. Heise, *Cleveland*

Paul S. Brallier, *Niagara Falls*

Oliver Osborn, *Houston*

Earl A. Gulbransen, *Pittsburgh*

A. C. Holm, *Canada*

J. W. Cuthbertson, *Great Britain*

T. L. Rama Char, *India*

●

ADVERTISING OFFICE

Jack Bain

Advertising Manager

545 Fifth Avenue

New York 17, N. Y.

Phone—*Murray Hill 2-3345*

Journal of the

Electrochemical Society

SEPTEMBER, 1953 VOL. 100 · NO. 9

CONTENTS

Regional Features

The Phenomenon of Southern California—Its Growth and Electrochemical Future—Editorial. *Joseph C. Schumacher* 245C
The Southern California-Nevada Area. *Joseph C. Schumacher* 247C

Technical Papers

Factors Affecting the Transformation to Gray Tin at Low Temperatures. *R. R. Rogers and J. F. Fydell* 383
Preparation of "Mischmetall" by Thermal Reduction. *C. Decroly, D. Tytgat, and J. Van Impe* 388
Studies on the Concept of Large Activator Centers in Crystal Phosphors
Part I. Dependence of Luminescent Efficiency on Concentration of Activator. Size of Luminescent Centers. *J. Ewles and N. Lee* 392
Part II. Effects of Concentration of Activator, of Temperature, and of Flux on the Excitation and Emission of CaO:Bi Phosphors. *J. Ewles and N. Lee* 399
Part III. Preparation and Properties of Calcium Oxide Phosphors with Eleven Different Activators. *J. Ewles and N. Lee* 402
Attempts at the Electrolytic Initiation of Polymerization. *H. Z. Friedlander, Sherlock Swann, Jr., and C. S. Marvel* 408
Structural Features of Oxide Coatings on Aluminum. *F. Keller, M. S. Hunter, and D. L. Robinson* 411

Feature Section

Utility Steam-Electric Stations—Summary of Development in the United States. *Louis Elliott* 261C
Electrochemical Entomology 264C

Current Affairs

Wrightsville Beach Technical Program 265C
Highlights of the Board of Directors' Meeting 270C
News Notes 267C
Section News 268C
Personals 269C
New Members 269C
New Products 272C
Employment Situations ... 272C

Published monthly by The Electrochemical Society, Inc., Mount Royal and Guilford Aves., Baltimore 2, Md., combining the JOURNAL and TRANSACTIONS OF THE ELECTROCHEMICAL SOCIETY. Editorial offices: 216 West 102nd Street, New York 25, N. Y. Statements and opinions given in articles and papers in the JOURNAL OF THE ELECTROCHEMICAL SOCIETY are those of the contributors, and The Electrochemical Society assumes no responsibility for them. Subscription $11.25 to members, $15.00 to nonmembers. Single copies $1.25 to members, $1.50 to nonmembers. Copyright 1953 by The Electrochemical Society, Inc. Entered as second-class matter November 15, 1947, at the Post Office at Baltimore, Md., under the act of August 24, 1912.

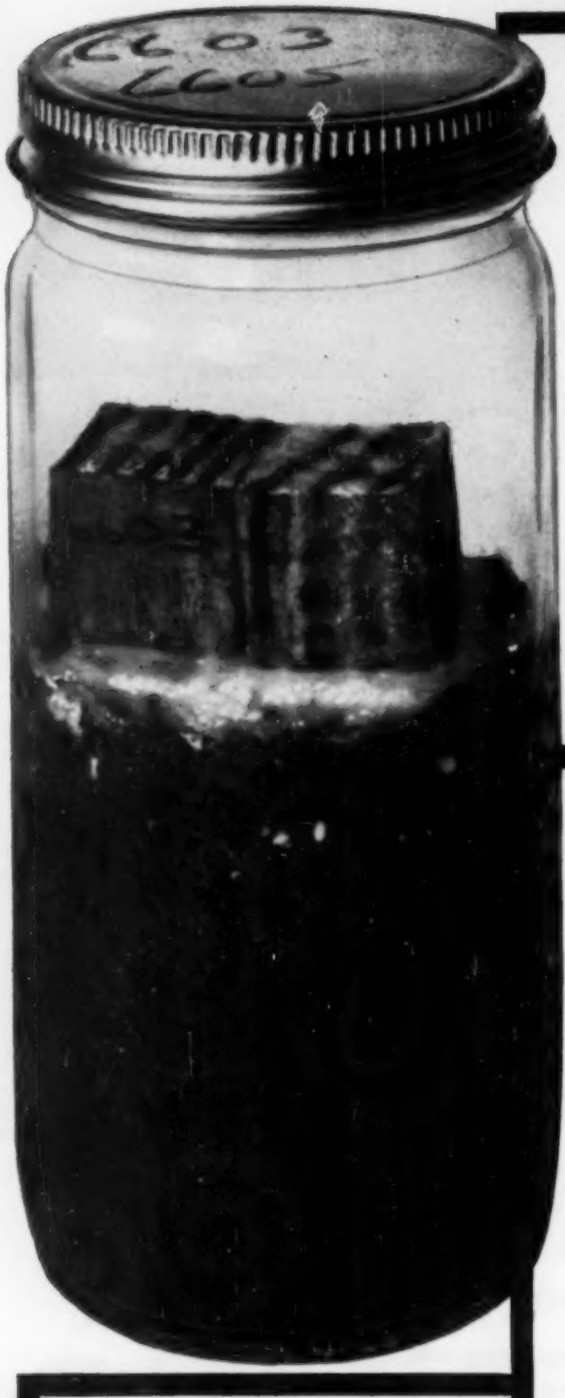

THIS BOTTLE TURNS SEVEN YEARS INTO SEVEN MONTHS

Test blocks of pole wood are fed to destructive fungi in bottles like this at Bell Laboratories. Wood rests on soil which controls moisture conditions and promotes fungus growth. Test speeds search for better preservatives.

This year the Bell System is putting 800,000 new telephone poles into service. How effectively are they preserved against fungus attack and decay?

Once the only way to check a preservative was to plant treated wood specimens outdoors, then wait and see—for seven years at least. Now, with a new test devised in Bell Telephone Laboratories most of the answer can be obtained in seven months.

Cubes of wood are treated with preservatives, then enclosed in bottles with fungus of the most destructive kind, under temperature and humidity conditions that accelerate fungus activity. Success—or failure—of fungus attack on cubes soon reveals the best ways to preserve poles.

The new test has helped show how poles can be economically preserved for many years. It is another example of how Bell Telephone Laboratories works to keep down the cost of your telephone service.

A boring is taken from a pole section to see how far preservative has penetrated. For poles to last, it must penetrate deeply and be retained for a long time.

BELL TELEPHONE LABORATORIES

Improving telephone service for America provides careers for creative men in scientific and technical fields

Factors Affecting the Transformation to Gray Tin at Low Temperatures[1]

R. R. Rogers and J. F. Fydell

Mines Branch, Department of Mines and Technical Surveys, Ottawa, Canada

ABSTRACT

The tendency for white tin, in the form of coatings and otherwise, to be transformed into gray tin is affected by the composition and thickness of the tin, the temperature at which transformation takes place, and the history of the tin prior to the transformation. Gray tin will appear spontaneously under certain conditions, and after inoculation with gray tin or germanium under other conditions. There should be little difficulty in preventing the formation of gray tin if certain precautions are taken.

Introduction

Ordinary white tetragonal tin may change into gray cubic tin at temperatures below 13.2°C (55.8°F) (see Fig. 1 and 2). This gray tin is cracked, brittle, and useless for most purposes. The term "tin disease" sometimes has been used in the literature when referring to this phenomenon, probably because of the wartlike appearance of the gray tin, to the way in which it spreads over the white tin surface, and to the fact that a sample of tin which is "infected" may cause other samples to become infected also. Even if gray tin is converted back into white tin by raising its temperature, the metal will continue to be porous and cracked until it has been remelted.

Gray tin occurrences have been mentioned in the literature from time to time. What is perhaps the first report was written in 1851 by Erdmann (1), who had found gray tin in organ pipes. Since that time a considerable amount of experimental work has been done in certain phases of this field, particularly by European investigators. As shown by a Mines Branch survey of the published work (2), comparatively little has been done since 1940.

Although the gray tin phenomenon is of no great practical interest in many countries, it is of considerable importance where the temperature is low during a large part of the year.

A paper has been published (3) on the effect of germanium on the transformation to gray tin. This paper summarizes the work done here to date on the effect of the composition and thickness of the tin, of the temperature at which the transformation takes place, and of the history of the tin prior to the transformation.

[1] Manuscript received January 20, 1953. This paper was prepared for delivery before the Montreal Meeting, October 26 to 30, 1952. Published by permission of the Deputy Minister, Department of Mines and Technical Surveys, Ottawa, Canada.

Three different types of tin were used: two (I and II) were obtained from ordinary commercial sources; the third (III) was produced in this laboratory by electrolytic refining. The composition of I is given in Table I; II was found by spectrographic means to be approximately the same as I except that it contained 0.015 per cent Sb and 0.009 per cent Pb; III was found by the same method to be lower than the other two with regard to each of the various constituents. In fact, the proportions of the more important impurities were so low they could not be determined readily.

All tin coatings were applied in the laboratory to iron-plated steel sheet samples, using the hot-dip method unless otherwise indicated. A molten flux consisting of the chlorides of zinc, sodium, and potassium was used. The steel sheet samples were plated with iron to prevent contact between the tin coating and the nonferrous constituents of the steel, which might have affected the experiments with gray tin.

Experimental

Early in the investigation it became important to find an adequate method for determining the rate of spread of gray tin. Most of the earlier investigators took advantage of the great volume increase (about 25%) accompanying the transformation, and determined the rate of spread by measuring the rate of volume increase. However, this method would be of little value in the case of very thin coatings such as those used in the present work, because the volume increase would be extremely small.

The authors have found that the relation

$$A^{\frac{1}{2}} = mT + b$$

exists where T is the number of days after inoculation required to produce a spot of gray tin having an area of A square millimeters, and b is a constant

for any particular spot. The value of m indicates the rate of spread.

The value of m is determined by measuring the area of the spot of gray tin at intervals under a low power microscope and then plotting $A^{\frac{1}{2}}$ against T. The slope of the straight line obtained is the value of m for the spot. When this value is 0.001, 0.01, 0.1, 1, or 10, an area of 1 cm² will be covered with gray tin at the end of 10,000, 1000, 100, 10, or 1 days, respectively, if the reasonable assumption is made that $b = 0$.

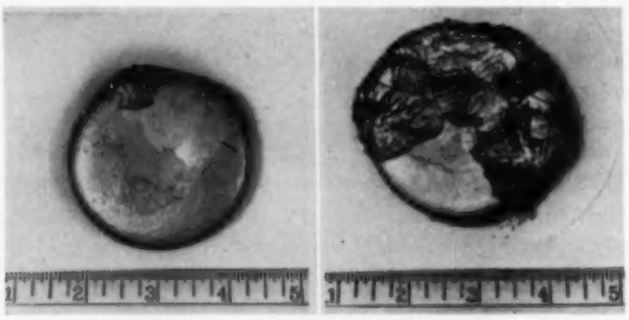

(*a*) (*b*)

FIG. 1. Button of type III tin. (*a*) 24 hr after inoculation; (*b*) 48 hr after inoculation.

FIG. 2. Typical spot of gray tin on an experimental coupon of tin-coated steel.

TABLE I. *Composition of type I tin*

	%		%
Antimony	0.0005	Iron	0.0002
Lead	0.0005	Silver	trace
Copper	0.0002	Sulfur	0.006
Bismuth	0.0002	Arsenic	trace

The value of b is the intercept of the straight line on the vertical axis. In these experiments it varied between −12.5 and 3.5, positive values being greatly in the majority. It is assumed that the value of b decreases as the area originally inoculated is decreased, and that the value is negative when the smallest possible area has been inoculated. On the basis of this assumption, there must always be an interval between the time of inoculation and the time of first appearance of the spot of gray tin.

A typical graph for a gray tin spot on a sample of tin-coated steel exposed to a temperature of −29°C (−20°F) is shown in Fig. 3. After the first six readings were taken, m was found to be 0.053. The temperature was raised to 4°C for approximately four days and then it was lowered again to −29°C. Seven more readings were taken, the m value being 0.051. These two values are considered to be identical within the accuracy of the experiment.

Effect of Composition

Sheet steel samples were electroplated with iron by a procedure described elsewhere (4). They then were hot-dip coated with type I tin containing various small proportions of one other metal (copper, zinc, lithium, magnesium, germanium, aluminum, silver, cadmium, or bismuth). Finally they were inoculated by pressing pieces of gray tin about the size of a pinhead into the tin coatings, the areas of

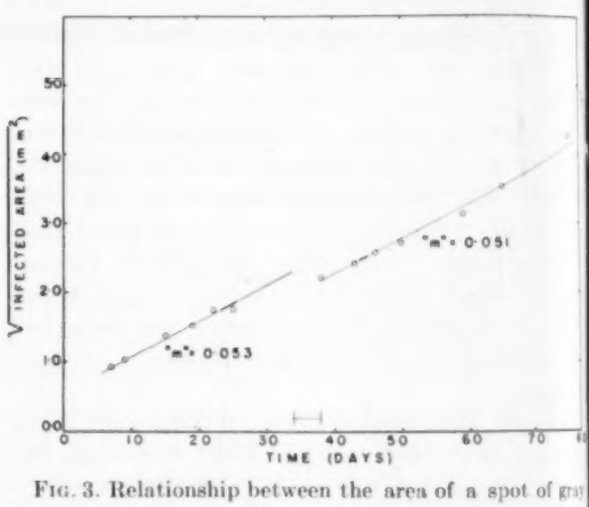

FIG. 3. Relationship between the area of a spot of gray tin and time after inoculation, in the case of a type I tin coating at −29°C (−20°F). (— —temperature at 4°C.)

contact between gray tin and white tin being extremely small. Some of the samples then were exposed to each one of the following temperatures: 4°, −29°, −40°, and −51°C. Gray tin was produced on all but a few of the samples and a wide variation in the rate of spread was observed. The m values obtained are given in Table II. The m value depends considerably on the composition of the tin. Certain added elements tend to increase the rate of spread and certain others tend to decrease it.

Similar samples were treated in the same way except that type II tin, with somewhat higher antimony and lead contents, was used in the coatings. Only additions of copper or zinc were made in these experiments, since these metals gave the highest m values when type I tin was used. The m values obtained are given in Table III. The higher antimony and lead contents caused a great decrease in m value.

Similar samples were prepared, using type I tin containing two added metals. The m values obtained in a number of cases are given in Table IV. The data in this table confirm that zinc and copper act as accelerators, and silver and bismuth as inhibitors. They also indicate that a certain metal can act as an accelerator or an inhibitor whether present alone or with other metals. Apparently there is a relationship between the m value and the concentration of the zinc in the tin.

TABLE II. *Values of m at different compositions and transformation temperatures, using type I tin*

Added metal	Concentration range of added metal (wt, %)	Average m value			
		at 4°C (+40°F)	at −29°C (−20°F)	at −40°C (−40°F)	at −51°C (−60°F)
Copper	0.001–0.15	—	0.342	0.322	1.64
Zinc	0.02–0.07	0.004	0.111	0.311	1.16
Lithium	0.0015–0.004	0.001	0.079	0.220	1.23
Magnesium	0.001–0.009	0.002	0.107	0.228	0.835
Germanium	0.009–1.10	—	0.054	0.178	1.09
Aluminum	0.0007–0.055	0.002	0.046	0.072	0.328
Silver	0.004–0.15	—	0.035	0.092	0.105
Cadmium	0.009–0.025	0.003	0.026	0.031	0.037*
Bismuth	0.003–0.27	—	0.017*	0.015*	0.118†
Type I tin alone		0.005	0.067	0.176	0.925

* On one sample, gray tin had not developed to any measurable extent and m value was rated zero. This was included when determining the average.

† On five samples, gray tin had not developed to any measurable extent and m value was rated zero. These were included when determining the average.

TABLE III. *Values of m at different compositions and transformation temperatures, using type II tin*

Added metal	Concentration range of added metal (wt, %)	Average m value		
		at −29°C (−20°F)	at −40°C (−40°F)	at −51°C (−60°F)
Copper	0.006–0.120	0.006	0.006	0.003
Zinc	0.016–0.057	0.005	0.004	0.004

Gray tin is not the only possible inoculating agent. In previous work (3) it was shown that elementary germanium may be used for this purpose.

A considerable part of the present investigation was devoted to a study of conditions under which gray tin would be produced spontaneously. In the earlier work (3), it was found that gray tin could be produced in this way in certain tin-germanium alloys. A very few cases of spontaneous formation were observed on the coatings listed in Table II, although these occurrences were very erratic.

Iron-plated steel sheet strips were coated in the same manner as the samples mentioned in Tables II, III, and IV and were then exposed to a temperature of −51°C for several hours. Finally they were bent through an angle of 90° and allowed to remain at that same temperature. Although no inoculation took place, gray tin appeared on the convex side, but not the concave side, of almost all of these samples (Fig. 4). The time which elapsed before the first appearance of the gray tin on the various samples is given in Table V.

TABLE IV. *Effect on the m value of adding two metals to type I tin simultaneously (transformation temperature −29°C or −20°F)*

Concentration of added metal (Wt, %)				m Value			
Zn	Cu	Ag	Bi	Zn	Zn + Cu	Zn + Ag	Zn + Bi
0.002			0.160	•			0.000
0.002			0.064				0.0006
0.003			0.038				0.002
0.010		0.023				0.004	
0.013		0.016				0.027	
0.019				0.130			
0.020		0.008				0.022	
0.022			0.002				0.006
0.032		0.005				0.011	
0.037				0.115			
0.043	0.001				0.090		
0.048		0.003				0.028	
0.050				0.020			
0.060	0.004				0.10		
Type I tin alone				0.07			

FIG. 4. Sample of tin-coated steel bent through 90°, showing gray tin at convex side of bend.

The accuracy of the m value was good in the case of each individual sample, as may be judged by an inspection of Fig. 3 and 5. The agreement between m values from samples which were supposed to be duplicates was less satisfactory. For that reason averages of m values from different samples are reported in this paper. Each of the values given in Tables II to V, inclusive, is an average of between 6 and 15 individual values. The difference between m values from supposedly duplicate samples

doubtless was due largely to the difficulty in controlling the thickness of the coatings.

Effect of Thickness

As shown in Table VI, the m value decreases as the thickness of the tin is decreased. Small experimental tin castings have been found to have m values as high as 27, which is much higher than the values

TABLE V. *Average time to first appearance of gray tin on bent samples coated with type I tin (transformation temperature −51°C or −60°F)*

Added metals	Concentration range of added metals (Wt, %)	Average time to first appearance of gray tin (days)
None		2
Copper	0.001–0.15	<1
Zinc	0.02–0.07	<1
Lithium	0.0015–0.004	<1
Magnesium	0.001–0.004	<1
Germanium	0.01–1.10	<1
Aluminum	0.0007–0.055	2
Silver	0.004–0.15	2
Cadmium	0.009–0.025	6
Bismuth	0.003	<1
	0.005	5
	0.006	28
	0.024–0.270	>42

TABLE VI. *Variation of m with coating thickness*

Nature of coating	Coating thickness (in.)	m
Commercial tin (electrolytic)	0.00004	0.005
Type I tin containing trace of lithium (hot dip)	(1) 0.00029 (2) 0.00032	0.07 0.09
Type I tin containing trace of magnesium (hot dip)	(1) 0.00027 (2) 0.00035	0.06 0.07
Type I tin containing trace of aluminum (hot dip)	(1) 0.00027 (2) 0.00032	0.04 0.06
Type III tin with no addition (hot dip)*	(1) 0.00027 (2) 0.00043	0.21 1.60

* Transformation temperature −40°C; in all other cases −29°C.

obtained in the case of any of the coatings investigated. The castings which gave this value were of type III tin.

Effect of Transformation Temperature

The effect of transformation temperature on the m value of tin coatings containing small amounts of other metals is shown in Tables II, III, and IV.

The authors were unable to obtain m values at 4°C, which was only about 9° below the critical temperature, because no inoculation took place. However, good results were obtained when a similar set of samples was inoculated and exposed to a temperature of −29°C until gray tin had appeared.

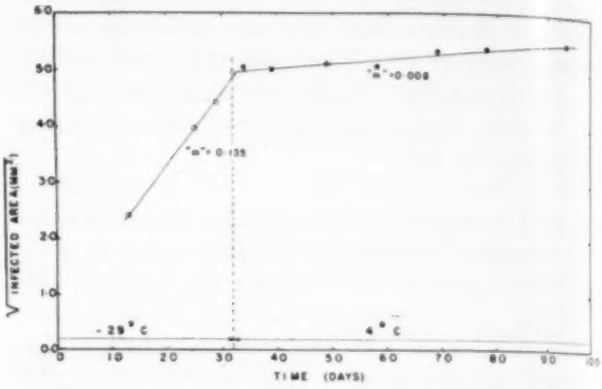

FIG. 5. Illustration of method of obtaining m value at a temperature near the critical temperature.

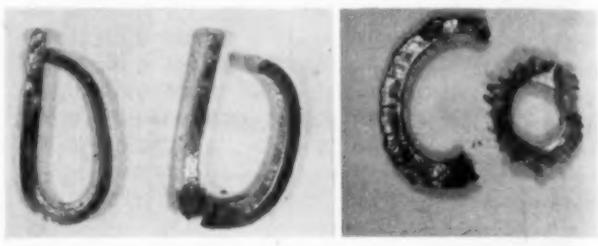

(*a*) (*b*) (*c*)

FIG. 6. Cast bar of type I tin, cooled to −29°C, bent, and maintained at that temperature. (*a*) Immediately after bending; (*b*) several months after bending; and (*c*) several days after (*b*).

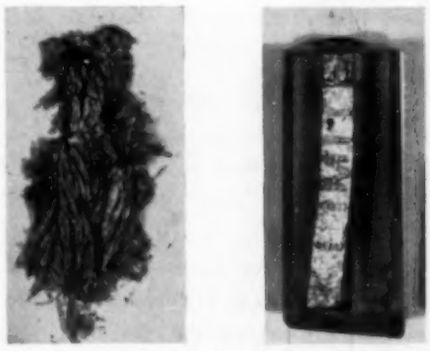

(*a*) (*b*)

FIG. 7. Cast bar of type I tin, cooled to −29°C, inoculated, and maintained at that temperature for 1 week. (*a*) Bar not encased; (*b*) bar encased in Lucite plastic, except at top end.

The temperature then was raised to 4°C and maintained there while values of m were obtained This method of obtaining m values at temperatures approaching the critical temperature is illustrated in Fig. 5.

Effect of History Prior to Transformation

A few examples of the effect of the history of the tin prior to transformation are given below.

It already has been shown that gray tin appeared spontaneously on the convex, but not on the concave, sides of steel samples which had been coated with type I tin, cooled to a suitable temperature, and then bent through 90°. When cast bars of type I tin were cooled to −29°C, bent through approximately 180°, and maintained at that temperature for several months, gray tin was produced spontaneously on the convex sides of the bends in four cases out of five. However, no change took place on the concave side of any of the bars (see Fig. 6).

These experiments indicate that the tendency to form gray tin is increased when the tin is placed in tension, but not when it is placed in compression. It is interesting to note that Hedges and Higgs (5) have reported they were able to produce gray tin by placing cylinders of white tin 0.25 in. in diameter and 0.25 in. high under a comparatively great weight of four tons while surrounded by solid carbon dioxide.

A 2-in. length of a cast bar of type I tin was completely converted to gray tin after it had been inoculated and exposed to a temperature of −29°C for one week (see Fig. 7*a*). A similar sample was completely encased in Lucite plastic except at one end and then treated in the same way. At the end of a week only the small part of the tin that had been exposed had been converted to gray tin (see Fig. 7*b*). Evidently, encasing the white tin in Lucite had prevented the expansion which accompanies the transformation and thus had prevented the transformation from taking place.

Conclusions

The data presented show that the tendency for white tin to be transformed into gray tin is affected by the composition and thickness of the tin, the temperature at which the transformation takes place, and the history of the tin prior to the transformation. In the experiments described, the value of m (the rate of spread) varied between 0.000 and 27.

It was shown, further, that gray tin appears spontaneously under certain conditions, and after inoculation with gray tin or germanium under other conditions.

It was concluded that, although gray tin may be produced under a wide variety of conditions, there should be no difficulty in preventing its formation in important amounts (*a*) if the conditions are adjusted so that the value of m is negligible; and/or (*b*) if inoculation is prevented by means of a suitable surface coating, and conditions are arranged so that gray tin is not produced spontaneously.

Any discussion of this paper will appear in a Discussion Section, to be published in the June 1954 issue of the Journal.

References

1. O. L. Erdmann, *J. Prakt. Chem.*, **52**, 428 (1851).
2. R. R. Rogers and W. R. G. Stewart, Investigation No. MD2609, Mines Branch, Department of Mines and Technical Surveys, Ottawa, Canada, Nov. 23, 1949. (Available on request.)
3. R. R. Rogers and J. F. Fydell, *J. Electochem. Soc.*, **100**, 161 (1953).
4. R. R. Rogers, *Ind. Eng. Chem.*, **27**, 785 (1935).
5. E. S. Hedges and J. Y. Higgs, *Nature*, **169**, 621 (1952).

Preparation of "Mischmetall" by Thermal Reduction[1]

C. Decroly and D. Tytgat

University of Brussels, Brussels, Belgium

and

J. Van Impe

Institut Interuniversitaire des Sciences Nucléaires, Brussels, Belgium

ABSTRACT

A method of preparation of "mischmetall" by thermal reduction of mixed fluorides of rare earth metals, using calcium as reducing agent, has been submitted to an experimental investigation. Raw materials were ores from the Belgian Congo from which, by using well-known chemical methods, mixed oxides of rare earth were extracted.

The preparation of the mixed fluorides was carried out in two steps. First, double fluorides of rare earth and ammonium were produced by reaction of the mixed oxides with ammonium bifluoride; then the double fluorides were decomposed by heating; ammonium fluoride being volatilized, the mixed fluorides can be easily recovered.

The mixed fluorides were submitted to thermal reduction with calcium with addition of a small amount of iodine. The reaction is self-supporting and small ingots of mischmetall were obtained with a fairly good efficiency.

Introduction

Methods of preparation of rare earth metals, either pure or alloyed, have been the subject of a good many investigations (1). Most of the researches carried out up to now have dealt with electrochemical processes. Fused salt electrolysis has been used commercially to produce mischmetall. However, thermal processes have been studied in recent years with some success.

It is well known that thermal reduction of rare earth metals is possible only by using other metals as reducing agent. These metals must have a greater affinity for oxygen or the halogens than do the metals to be produced. In the case of oxides of rare earth metals, reduction with elements such as calcium, barium, magnesium, or aluminum gives only a mixture of oxides and metals which are not easily separable (2). When chlorides are used, results are better but not completely satisfactory, as rare earth chlorides are difficult to prepare free from oxychlorides and are very hygroscopic.

Moldenhauer, in 1914 (3), carried out some experiments on reduction of cerium trifluoride with calcium. He could only obtain an alloy of cerium and calcium with 12 per cent calcium. More recently, Mahn (4, 5) investigated the reduction of mixed rare earth fluorides using liquid magnesium at 800°C with addition of chloride fluxes. Only alloys containing up to 20 per cent magnesium could be obtained with an efficiency lower than 30 per cent. Gray (6) has prepared very pure cerium by reduction of cerium trifluoride with lithium, using iodine as a booster. The reductions were carried out in a steel bomb with external heating. Efficiencies as high as 82 per cent were attained.

The purpose of this investigation was to see whether it was possible to prepare mischmetall starting with mixed rare earth fluorides by using a self-supporting reaction without any external heating. Having obtained very good results with this kind of reaction when reducing uranium tetrafluoride with calcium (7), it was thought that the investigation was worthwhile in the case of rare earth metals as the operation can be carried out in a very simple way.

Experimental

Preparation of mixed rare earth oxides.—Ores came from the Belgian Congo. Samples of bastnasite, rare earth fluorocarbonate, and of monazite were used. Conventional chemical methods were used to separate the mixed oxides, but the experimental work was rather arduous.

Preparation of mixed rare earth fluorides.—To avoid using hydrofluoric acid or fluorine, both of which are toxic and very corrosive, ammonium bifluoride was employed as a fluorination medium. As has been known since Berzelius and Marignac, ammonium difluoride is a good fluorination agent for oxides such as ZrO_2 or BeO. This method was tried with the mixed rare earth oxides with good results.

[1] Manuscript received April 28, 1952. This paper was prepared for delivery before the Philadelphia Meeting, May 4 to 8, 1952.

The preparation of mixed fluorides is carried out in two steps. First, an intimate mixture of rare earth oxides with an excess of ammonium bifluoride is heated for several hours at 150°C. The reaction between ammonium bifluoride and a rare earth oxide of type X_2O_3 may be written

$$X_2O_3 + 4NH_4F \cdot HF \rightarrow 2XF_3NH_4F + 2NH_3 + 3H_2O.$$

The result of this first operation is, therefore, a mixture of double fluorides of rare earth and ammonium which remain as solids in the fluorination apparatus, ammonia and water vapor being free to escape.

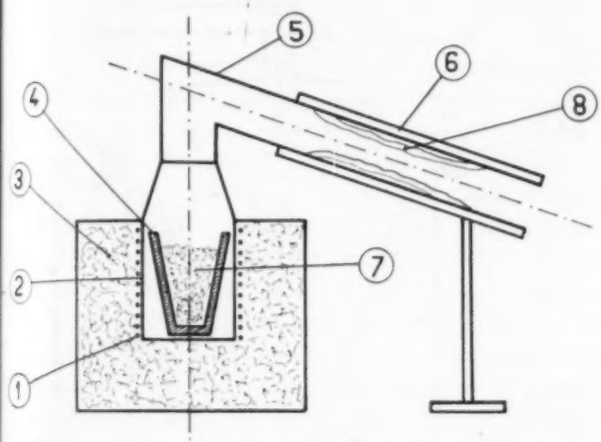

FIG. 1. Schematic diagram of apparatus used in the preparation of mixed fluorides. 1—heating coil; 2—copper vessel; 3—heat insulation; 4—aluminum crucible lined with sintered calcium fluoride; 5—copper or aluminum collector; 6—silica tube; 7—charge, mixture of rare earth oxides and ammonium bifluoride; 8—condensed ammonium fluoride.

The apparatus used to carry out this preparation is shown schematically in Fig. 1.

The charge to be treated is placed in a crucible, such as one of aluminum lined with slightly sintered calcium fluoride. This crucible is put in an electric furnace and a copper or aluminum collector is put over the crucible to recover the gases evolved by the reaction. The collector is connected with a silica tube where some volatilized ammonium fluoride can be condensed and recovered. No attempts were made in our experiments to recover ammonia, but this could have been done without difficulty. The temperature is kept constant within a few degrees; the reaction proceeds smoothly and need not be watched.

The second step of the preparation is the decomposition of the double fluorides by heating. On heating, the following reaction occurs

$$XF_3NH_4F \rightarrow XF_3 + NH_4F.$$

To get complete decomposition within a reasonable time, the temperature must be raised to 400°C. Moreover, in order to avoid formation of any oxyfluorides by action of atmospheric oxygen and water vapor, the decomposition must be carried out either under vacuum or under inert dry atmosphere. Both methods were tested and either can be used. However, simplicity of apparatus favors decomposition in an inert dry atmosphere as, in this case, no pumping system is necessary.

Fig. 2 shows schematically the apparatus used to carry out the decomposition. A silica tube which can be placed in an electric furnace serves as decomposition vessel. This tube is connected to another silica tube by a rubber connection. The second tube serves as a condenser and can be cooled with a copper coil in which water can be circulated. To carry away ammonium fluoride vapors and to keep an inert atmosphere in the apparatus, dry nitrogen can be introduced in the decomposition tube. Ammonium fluoride condenses in the condensation tube and can be easily recovered.

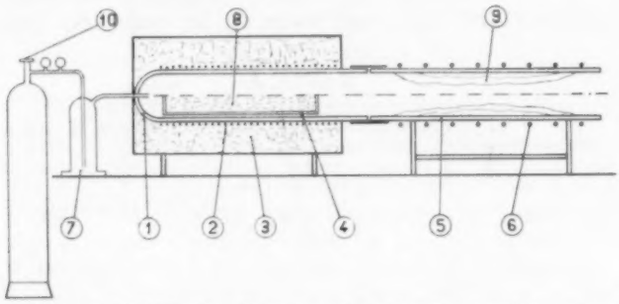

FIG. 2. Schematic diagram of apparatus used to carry out the decomposition. 1—decomposition tube; 2—heating coil; 3—heat insulation; 4—alumina trough lined with calcium fluoride; 5—condenser; 6—copper coil; 7—wash bottle; 8—charge; 9—condensed ammonium fluoride; 10—nitrogen tank.

The charge of double fluorides is placed in an aluminum trough lined with calcium fluoride and the trough placed in the decomposition tube. Temperature is raised to 400°C and nitrogen is kept flowing at a slow rate in order to avoid losses of ammonium fluoride in the condenser. Under these conditions, decomposition of a charge of 1000 grams takes 10 to 12 hours. Complete elimination of ammonium fluoride is checked by determining the nitrogen content of the finished product. Decomposition is considered finished when the nitrogen content is less than 10 ppm. Chemical analysis for fluorine showed that rare earth elements are all present as trifluoride.

Thermal Reduction of Mixed Rare Earth Fluorides

Theoretical considerations.—Table I gives values of the heat evolved in reactions of the type shown:

$$2XF_3 + 3Ca \rightarrow 2X + 3CaF_2.$$

These are computed on the basis of one gram atom of halogen using the heats of formation at 298°K of the halides as they are given by Quill (8). It can be seen that in the case of trifluorides only calcium gives exothermic reactions and that the heat evolved is not very high. For example, the reduction of CeF_3 with calcium

$$2CeF_3 + 3Ca \rightarrow 2Ce + 3CaF_2$$

yields $\Delta H_{298} = -38.4$ kcal. This value is rather low. If cerium were tetravalent, more heat would be evolved but, unfortunately, CeF_4 is very difficult to prepare and does not seem to be stable at high temperature. When starting with a mixture of trivalent fluorides, the composition of which is such as to obtain an alloy containing 50 per cent Ce, 30 per cent La, and 20 per cent Nd, it can be shown that the heat evolved per gram atom of fluorine is only −6.3 kcal.

TABLE I

Rare earth halide	Reducing metal ΔH_{298} in kcal per gram atom of halogen				
	Ca	Mg	Na	K	Al
$CeCl_3$	−8.6	+10.0	−11.6	−17.7	+31.0
$LaCl_3$	−7.3	+11.4	−10.3	−16.4	+32.4
$NdCl_3$	−10.6	+8.0	−13.6	−19.7	+29.0
CeF_3	−6.4	+7.1	+2.6	+4.1	+31.0
CeF_4	−34.6	−21.0	−25.5	−24.0	+2.8
LaF_3	−4.7	+8.8	+4.3	+5.8	+32.6
NdF_3	−8.4	+5.1	0.0	+2.1	+31.1

A very approximate calculation of the theoretical temperature which could be reached without any external heating shows that with such a low available heat it is impossible to melt the reduced metals and the slag.

At first sight, reduction of fluorides with calcium without external heating would appear impracticable. There is, however, the possibility of using a booster as is sometimes done in aluminothermic processes. In that case, some oxygenated compound is added to the charge in order to get more heat. Compounds such as potassium chlorate may be used as they give off their oxygen very easily on heating. Higher temperature can be reached and, consequently, metal and slag can be melted and separated. Examples of such procedure are given by Burchell (9). In the case of reduction of fluorides, addition of oxygenated compounds does not seem advisable as there is a danger of oxidizing the reduced metal.

Spedding and his coworkers (10, 11) have shown that iodine could be used as supplementary fuel when the heat evolved by the main reaction is not sufficient to melt the metal and the slag. Moreover, when using iodine as booster and calcium as reductor, calcium iodide is formed, and the mixture of calcium iodide and calcium fluoride melts at a lower temperature than pure calcium fluoride; therefore, separation of metal and slag will be much easier. McKechnie and Seybolt (12) have shown that addition of iodine was advisable when reducing oxides such as V_2O_5.

Experimental procedure.—Fig. 3 shows schematically the apparatus used to carry out the reduction of mixed rare earth fluorides with calcium. It consists of a steel pot provided with a removable lid. In order to get air tightness when the lid is in its closing position, a water-cooled circular rubber gasket is used. This gasket is placed in a circular trough, welded at the top of the steel pot.

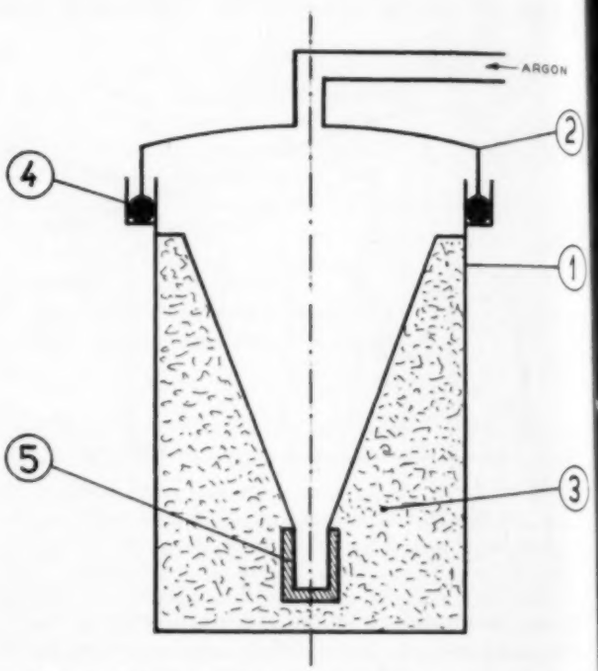

FIG. 3. Schematic diagram of apparatus used to carry out the reduction of rare earth fluorides with calcium. 1—steel pot; 2—removable lid; 3—packed calcium fluoride; 4—rubber gasket; 5—collecting crucible of sintered calcium fluoride.

The reaction chamber is conical, but at the bottom of this chamber there is a cylindrical crucible of sintered calcium fluoride which serves as metal collector. The wall of the reaction chamber is made of packed calcium fluoride powder. In order to dry completely the lining and the crucible before an operation, an electric heating coil is provided in the pot. Perfect dryness of the lining is necessary to get satisfactory results. The use of pure calcium fluoride as refractory material is advisable as there will not then be any danger of contamination of the produced metal except by elements already present in the charge.

Reduction experiments were carried out in the following way. First, mixtures of thoroughly dried mixed rare earth fluorides with calcium chips were used but, with such charges, no satisfactory results could be obtained. Then experiments were performed with addition of iodine to the mixture of fluorides and calcium. After several trials, it was found that the best results could be obtained when using a mixture of 150 grams of mixed fluorides, 70 grams of iodine and an amount of calcium chips 15 per cent in excess of the quantity theoretically needed to reduce the fluorides and to combine with iodine.

Ingredients of a charge are mixed in a glass bottle and the mixture is then placed in the reaction vessel. The reaction is started with an inflamed magnesium ribbon and proceeds very smoothly, almost without spattering, and lasts only a few seconds. When the reduction is through, the vessel is closed with the lid. The lid is provided with a tube which allows pumping off all the air present in the reactor and replacing it by pure argon. During the cooling of the reaction products, a pressure of argon slightly greater than atmospheric pressure is maintained in the reactor. After cooling, the reactor is opened and the products are recovered. Separation of slag and metal is easily done since the metal collects in the lower crucible as a small ingot.

With charges of the composition given, efficiencies of 78 to 80 per cent could be obtained which is a fairly good result for small charges. For larger charges, efficiencies would probably be much better.

As the purification of the mixed rare earth fluorides was not perfect, the mischmetall obtained was still comparatively impure, as shown by the following analysis:

Rare earth metals:	98.2% (47.9% Ce, 50.3% La, Nd, etc.)
Calcium	0.32%
Silicon	0.09%
Iron	1.04%
Copper	0.28%
Not determined	0.07%

Such a metal can be used to prepare pyrophoric alloys. The content of calcium is still noticeable but most of it could probably be distilled off by vacuum melting.

Conclusions

Small ingots of mischmetall have been produced by thermal reduction of mixed rare earth fluorides with calcium, using iodine as a booster in order to have a self-supporting reaction without any external heating. Efficiencies are fairly good on a small scale and simplicity of the method is very attractive. Commercial feasibility of this method depends on the prices of calcium and iodine. At the present time, thermal reduction for production of mischmetall seems to be more expensive than electrolytic reduction but this might change if calcium could be produced at a lower price.

Acknowledgment

The authors wish to thank the Nuclear Physics Center of the University of Brussels, and the Belgian "Institut Interuniversitaire des Sciences Nucléaires" for financial help.

Any discussion of this paper will appear in a Discussion Section, to be published in the June 1954 issue of the Journal.

REFERENCES

1. F. Trombe, *Ann. chim. Paris*, **6,** 349 (1936).
2. F. Trombe, *Tech. mod.*, **30,** 855 (1938).
3. M. Moldenhauer, *Chem. Ztg.*, **38,** 147 (1914).
4. F. Mahn, *Compt. rend.*, **228,** 1298 (1949).
5. F. Mahn, *J. recherches centre natl. recherche sci. Labs. Bellevue, Paris*, **10,** 28 (1950).
6. P. M. J. Gray, *Metal Ind. London*, **80,** 43 (1952).
7. C. Decroly and J. Van Impe, *Bull. tech. AIBr.*, **3,** 205 (1950).
8. L. L. Quill, "The Chemistry and Metallurgy of Miscellaneous Materials. Thermodynamics," p. 79, McGraw-Hill Book Co., Inc., New York (1950).
9. T. Burchell, "The Aluminothermic Process," in "The Refining of Nonferrous Metals," p. 484, Institution of Mining and Metallurgy, London (1950).
10. F. H. Spedding, H. A. Wilhelm, W. H. Keller, and D. Peterson, U. S. Atomic Energy Commission, M.D.P. Report CT 816, July 1943.
11. F. H. Spedding, H. A. Wilhelm, and W. H. Keller, U. S. Atomic Energy Commission, MDP Report CT 2712, June 1945.
12. R. K. McKechnie and A. V. Seybolt, *J. Electrochem. Soc.*, **97,** 311 (1950).

Studies on the Concept of Large Activator Centers in Crystal Phosphors

I. Dependence of Luminescent Efficiency on Concentration of Activator. Size of Luminescent Centers[1]

J. Ewles and N. Lee[2]

Department of Physics, The University of Leeds, Leeds, England

ABSTRACT

The explanation of the variation of efficiency with concentration of activator in terms of a large center, given by Ewles, was oversimplified. The recent suggestion of Johnson and Williams that an activator can only function as a luminescent center if no other activator occupies any of Z lattice sites surrounding it, leads to the same expression for the number of centers as that originally given by Ewles and is effectively based on the same idea. Making use of the experimental findings reported in the present work that lattice defects can act as luminescent centers, and taking into account the competition of these centers in the luminescent process, a modification of Ewles' theory of efficiency based on the idea of a large center leads to the expression

$$E = K/(1 + \alpha c^{-1} \exp nc)$$

for the efficiency. The preparation of two series of calcium oxide phosphors from highly purified and annealed calcium oxide is described. The modified theory is shown to agree well with efficiency measurements on these phosphors and with those quoted by Johnson and Williams, except at high concentrations. Estimates of the "radial extent" of the centers are given.

Introduction

Lenard (1) suggested that in an impurity-activated phosphor the luminescent center consists of an atom of impurity linked with a number of host atoms; he attributed each emission band to a different center. Ewles (2), using the idea of a large center, consisting of an atom or ion of activator associated with a number n of host ions and assuming random distribution, showed that the fraction of such centers for an atomic concentration c of activator would be $c/(1 + c)^{-n}$, or, if c is small, $c \exp(-nc)$. Assuming further that the absorption both for emitted and exciting light is small for very thin layers of phosphors, Ewles showed that the luminescent efficiency of such layers could be expressed as $E = Ac \exp(-nc)$.

Some experimental evidence was given in support of this, and an estimate of the size of the center obtained. Recent experiments have shown, however, that it is impossible to obtain in practice layers thin enough to justify the assumptions of small absorption. The agreement between the oversimplified theory and the experimental results probably represented special cases of a more general theory of efficiency. Johnson and Williams (3), apparently unaware of the previous work, have recently developed a similar theory. They postulate that the luminescent center is an activator atom or ion having no other activator atom or ion of the same kind within Z nearest lattice positions, and arrive at the expression $c(1 - c)^z$ for the fraction of activators functioning as radiative centers. This expression, provided c is small, as it usually is, is identical with that previously obtained by Ewles and is, of course, based on the same idea. Johnson and Williams, by considering the effect of absorption (or what is effectively the same thing, capture cross section) of the radiative centers, nonradiative centers, and host ions for both exciting and emitted light, arrive at the expression

$$\eta = \frac{c(1-c)^z\sigma'}{(1-c)\sigma + c(1-c)^z\sigma' + c[1-(1-c)^z]\sigma''}$$

for the luminescent efficiency, where σ', σ'', and σ involve the capture cross sections of radiative, nonradiative centers, and host ions, respectively. In order to reduce this to a form more amenable to experimental test, they further assume that $\sigma' = \sigma''$, i.e., that the capture cross sections of radiative and nonradiative centers are the same. The luminescent efficiency then becomes

[1] Manuscript received May 12, 1952. This paper was prepared for delivery before the Philadelphia Meeting, May 4 to 8, 1952.

[2] Present address: City of Gloucester Technical College, Gloucester, England.

$$\eta = \frac{c(1-c)^z}{c + \frac{\sigma}{\sigma'}(1-c)}.$$

By comparing this with experimental results for the phosphors KCl:Tl, ZnF_2:Mn, and ZnS:Cu they obtain, after suitable choice of Z and σ/σ', fair agreement with experiment, except in some cases at higher concentrations and in other cases where the experimental points are too scattered to make convincing comparison. Johnson and Williams report from measurements of absorption by Parkinson and Williams (4) on MnF_2 and ZnF_2:Mn, and on KCl:Tl and TlCl, experimental justification of the assumption that the capture cross sections of radiative and nonradiative activators are of similar magnitudes. It is difficult, however, to accept this assumption as generally valid, for experiment indicates (see Part III) that excitation of luminescence is generally specific to the center and, except in special cases, unlike the normal absorption of the activator ions. It is suggested that both treatments require modifications.

Modified Theory of Efficiency

The real crystals which constitute the matrix of phosphors have generally been subjected to heat-treatment. This will result in the formation of lattice defects which may include vacant lattice sites, interstitial ions or atoms, and regions of strain. In addition, there will be, in the microcrystalline mass, surface levels at which electrons may be trapped and excited. In the section of this communication dealing with the preparation of pure nonluminescent calcium oxide it is reported that sudden cooling or grinding will produce luminescence in highly purified calcium oxide which, on slow cooling, is nonluminescent. Similar results have been obtained in this laboratory with many other substances. These observations indicate that lattice defects can act as luminescent centers and presumably, in some cases, as quenching centers. It is clearly necessary in any consideration of the luminescent efficiency of real crystals to take into account such centers, which now will be called structure centers.

The following assumptions will now be made: (*a*) the activator centers and structure centers are both large, i.e., several lattice parameters in extent; (*b*) the exciting radiation will be absorbed appreciably by both kinds of centers, but to different extents; this is in accord with the Johnson and Williams concept of the role of competing processes; (*c*) the absorption of the ideal lattice and nonradiative activators is negligible both for exciting and emitted radiation; (*d*) the activator will not function as a luminescent center if perturbed by the overlap of another center; (*e*) the concentration of the structure centers is approximately the same in phosphors with the same host and prepared by the same heat-treatment.

Suppose that in unit volume of the phosphor there are a total of N lattice sites of which A are occupied by activator atoms and S rendered unavailable for radiative activators by structure defects. Consider successive cation sites 1, 2, 3, etc. The probability that site 1 is occupied by an activator is A/N. The chance of site 2 being occupied by a host cation unperturbed by a structural defect is $(N\text{-}S\text{-}A)/N$. The chance of an activator occupying a site surrounded by n normal host cations is therefore

$$(A/N)[(N - S - A)/N]^n = c[1 - c' - c]^n.$$

Since c' and c are small compared with unity and c' is assumed constant for series of phosphors prepared under similar conditions, the number of radiative activator centers per unit volume is, therefore,

$$Nc(1 - c' - c)^n = Nc \exp[-n(c' + c)]$$
$$= NcB \exp(-nc)$$

where B is a constant $= \exp(-nc')$. This is the same expression as that originally deduced by Ewles. But the assumption made by him regarding absorption can no longer be retained. Consider a layer of the phosphor of thickness t and of unit area illuminated by exciting light of intensity I_0. The intensity of exciting light reaching a layer of thickness dy at a depth y below the surface is

$$I = I_0 \exp -[f_1 NcB \exp(-nc) + f_2 Nc']y$$

where f_1 and f_2 are the absorption coefficients for activator and structure centers, respectively, and c' is the concentration of structure centers. The luminescent intensity emitted by this layer dy at depth y is, therefore,

$$dL = pINcB \exp(-nc)dy$$

where p is the efficiency of excitation of the radiative centers. If the light emitted is in the visible or near ultraviolet, it may be assumed that the absorption by the host and the structure centers is negligible. For small concentrations, absorption of emitted light by activators may also be neglected. Hence the contribution of the layer to the total luminescence emitted on the side toward the incident exciting light is

$$dL = pI_0 NcB \exp(-nc) \exp -[f_1 NcB \exp(-nc) + f_2 Nc']y \cdot dy$$

Integrating through the whole thickness t the total intensity at the surface is

$$L = \frac{pI_0 NcB \exp(-nc)}{f_1 NcB \exp(-nc) + f_2 Nc'}[1 - \exp(f_1 NcB \exp(-nc) + f_2 Nc')t].$$

Experience shows that the absorption of the exciting light is complete in the thinnest layers practicable. This makes the exponential term in the square brackets zero so that we now have

$$L = \frac{pI_0NcB \exp(-nc)}{f_1NcB \exp(-nc) + f_2Nc'}$$

or writing $\eta = L/I_0$ for the effective luminescent efficiency and dividing throughout by $NcB \exp(-nc)$

$$\eta = p/[f_1 + (f_2c'/B)c^{-'} \exp(nc)].$$

Taking into account that what is actually measured is a number E proportional to the efficiency, the final expression becomes

$$E = K/[1 + \alpha c^{-1} \exp nc]$$

where K is a normalizing constant and $\alpha = f_2c'/f_1B$. Differentiating this expression with respect to c gives an optimum concentration at $c = 1/n$, a fact that permits the evaluation of n, the number of lattice ions associated with the radiative centers, from the experimental determination of the optimum.

Experimental Determination of Dependence of Efficiency on Concentration of Activator

Preparation of Nonluminescent Calcium Oxide

The experimental problem involves the preparation of a series of phosphors of different and known concentrations of activator in a host which, after the same heat-treatment without activator, shows little or no luminescence itself. Ewles and Curry (5) have shown that "Specpure" CaO gives an ultraviolet luminescent band whose characteristic resolved structure is identical with that given after activation by Pb. The removal of this Pb band requires a very high degree of purity of the base material. In the present work, purification was effected by dissolving A.R. grade $CaCO_3$ in doubly distilled nitric acid, repeated treatment of the solution with ammonium sulfide followed by filtration, fractional crystallization of calcium nitrate, and thermal decomposition of this nitrate in platinum vessels. The final product showed no trace of visible luminescence under strong ultraviolet excitation and no trace of the ultraviolet band which is found with as little as 10^{-6} atomic parts of Pb.

Preliminary trials had shown that the highly purified CaO prepared as above must be heated slowly in platinum vessels in order to obtain nonluminescent products. Heating in silica, alumina, or porcelain vessels gives a marked luminescence and, even in platinum vessels, rapid heating or cooling gives a product which shows a whitish luminescence, the spectral peak of which is at about 4500 Å. Crushing or grinding of samples rendered nonluminescent by slow heating and cooling again gives products showing this whitish luminescence. Samples rendered luminescent by rapid cooling or by crushing can be made nonluminescent again by repeated annealing at 1200°C. (These effects are considered in the Theoretical Discussion.)

To prepare the graded phosphors from the highly purified nonluminescent calcium oxide, about one gram of this was weighed out into each of nine small platinum thimbles. To each was added the appropriate amount of Specpure bismuth nitrate or lead nitrate solution. The thimbles were packed close together in an alumina container which was then placed in the middle of a large electric oven. The temperature was raised slowly to 700°C and so maintained for an hour. The temperature was then slowly lowered to about 80°C and the samples transferred to, and sealed into, tubes of clear nonfluorescent silica while still warm. Tests after similar heat-treatment of samples containing up to about 3 per cent Pb or Bi showed that the loss of activator on heating was negligible.

Measurement of Luminescent Efficiency

General Considerations

The measurements of the luminescence and of the exciting light were made with a photomultiplier operated from a stabilized power pack and coupled to a moving coil galvanometer. The linearity and steadiness of the arrangement were checked. Readings were found to be linear over a range greater than that required, and steady to about 1 per cent. The exciting source was a Mercra mercury vapor lamp operated from a large capacity battery of accumulators and cooled by a steady stream of air. No attempt was made to measure the absolute efficiency, for what was required in the present investigations was merely the variation of relative quantum efficiency with the concentration of activator. The readings corresponding to the luminescence were taken with a filter F_1 between source and phosphor which transmitted only a narrow spectral band of exciting light, and a complementary filter F_2 between phosphor and photomultiplier which transmitted only the luminescence (or a part of it) and cut off the exciting light (Fig. 1). At first it would appear that a reading corresponding to the exciting light could be obtained by replacing the filter F_2 by another filter like F_1, the signal then recorded being proportional to the excited light scattered from the phosphor and, therefore, to the excitation. But this would only be true if the absorption by the phosphor were the same for all concentrations. Clearly this cannot be so, for the efficiency does vary with concentration. However, the yellow light in the unfiltered source is not appreciably absorbed, except at concentrations of ac-

tivator so large that the efficiency is no longer of any interest. Hence a measure of the yellow light scattered from the phosphor is a measure of the relative exciting intensity. For this measurement then the filters F_1 and F_2 were replaced with those that transmit only the yellow lines of mercury (F_3). Allowance for scattered light was made in the following way. Let S_1 be the signal due to nonexciting scattered light when the luminescence being measured contributes a signal L, and S_2 the signal due to nonexciting scattered light when the source being measured contributes a signal I, after allowance has been made in all cases for the dark current. For pure CaO, prepared as described earlier, the luminescence is certainly zero, so that for such a sample the ratio of the signals is $S_1/(I + S_2)$. Then if $S_2 \ll I$, as is found to be the case, we have

$$\frac{L + S_1}{I + S_2} - \frac{S_1}{I + S_2} = \frac{L}{I + S_2} \approx L/I = E.$$

That is, the difference of the ratios of the two signals with phosphor and with pure CaO is a measure of the relative luminescent efficiency.

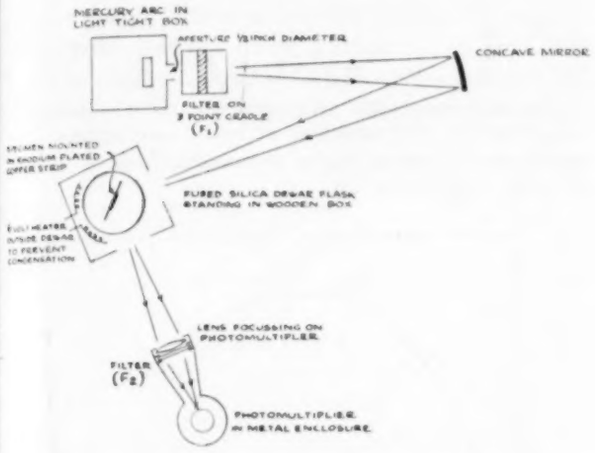
MERCURY ARC IN LIGHT TIGHT BOX
APERTURE ½INCH DIAMETER
CONCAVE MIRROR
FILTER ON 3 POINT CRADLE (F_3)
FUSED SILICA DEWAR FLASK STANDING IN WOODEN BOX
LENS FOCUSSING ON PHOTOMULTIPLIER
FILTER (F_2)
PHOTOMULTIPLIER IN METAL ENCLOSURE

FIG. 1. Arrangement of equipment for investigation of dependence of luminescent efficiency on concentration of activator.

Experimental Assembly

The general layout is shown in Fig. 1. The mercury arc is housed in a "uralite" box[3] with a ½-in. exit hole in front of which is the appropriate filter. The phosphor is held on a rhodium-plated copper strip by a crystal quartz plate and metal clip (Fig. 2), an approximately constant thickness of phosphor being obtained by use of a mica mask between copper and quartz plates. An image of the source exit hole is focused on the phosphor by means of an aluminized mirror, care being taken to avoid any illumination of the surroundings. The signal light from the phosphor is focused on the sensitive surface of the photomultiplier by a glass lens through the appropriate filter F_2. Since different parts of the photomultiplier surface are different in sensitivity, the image of the phosphor is made somewhat larger than this surface and any wandering is prevented by rigid mountings. From the preceding discussion of the principles of the measurements, it is seen that the filters must be changed between readings for luminescence and source. This change must be effected quickly so as to avoid as far as possible any change of dark current or any long-term drift of source intensity or photomultiplier sensitivity, and in such a way that the optical parts are not relatively displaced. Two cradles, each with 3 locating pins fitting hole, slot, and plane on rigid blocks, carry the filters. With this arrangement, changes of filter can be made rapidly and precisely. It was found that the readings corresponding to excitation or luminescence could be repeated to within 1 per cent. For work at various constant temperatures, the copper plate supporting the phosphor stands in a Dewar of transparent silica.[4] When the Dewar contains liquid oxygen, nitrogen, or hydrogen, the phosphor is just above the liquid surface. Condensation on the quartz plate is avoided by delaying immersion until the whole of the flask above the liquid is filled with dry gas. Condensation on the outside of the flask is prevented by a small heater. The temperature is measured by means of copper and constantan wires attached to the copper plate. A wooden rod fixed to this plate passes through a lid fitting a box holding the Dewar. A cross piece attached to the rod bears against pins in the lid so

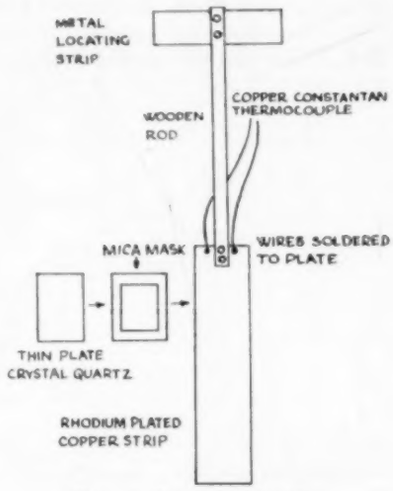

FIG. 2. Specimen holder

[3] "Uralite" is an asbestos and cement composition board.

[4] Through the courtesy of the Thermal Syndicate Ltd., a portion of this flask opposite the phosphor was made of nonfluorescent silica.

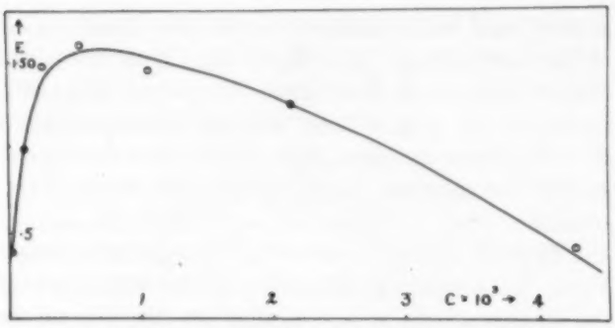

FIG. 3. Luminescent efficiency (arbitrary units) vs. concentration of activator. CaO:Bi. At −193°C. Low temperature band. ○ = experimental points; curve calculated from $E = K/(1 + \alpha c^{-1} \exp nc)$, with $n = 1250$, $\alpha = 1.17 \times 10^{-4}$, $K = 2.2$.

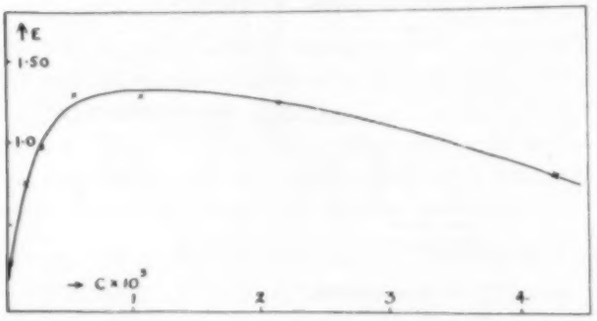

FIG. 4. Luminescent efficiency vs. activator concentration CaO:Bi at room temperature. X = experimental points; curve calculated from $n = 825$, $\alpha = 1.54 \times 10^{-4}$, $K = 1.75$.

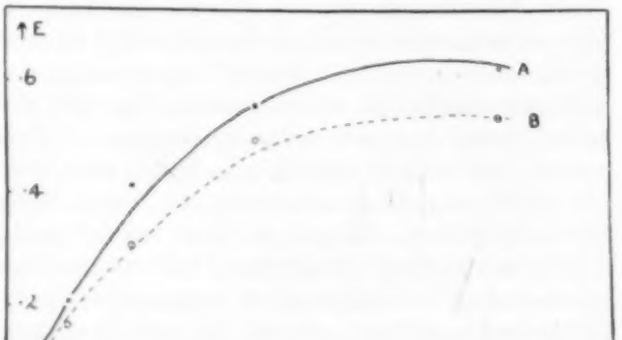

FIG. 5. Luminescent efficiency vs. activator concentration CaO:Pb. Yellow emission. X = room temperature, ○ −193°C—experimental points; curves calculated from A—$n = 250$, $\alpha = 0.056$, $K = 25$; B—$n = 250$, $\alpha = 0.052$, $K = 20$.

that the phosphor could always be replaced quickly in the same position. These arrangements insure that the same area of phosphor is imaged on the photomultiplier surface each time. The complementary nature of the filters F_1 and F_2 was tested by interchanging them, i.e., with F_2 (transmitting luminescence only) over the source and F_1 (transmitting exciting light only), over the photomultiplier. No signal was obtained in excess of that due to the small measured dark current.

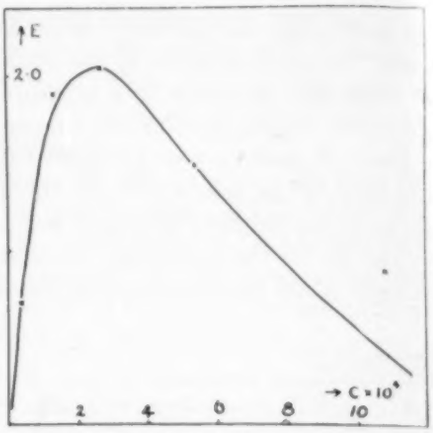

FIG. 6. Luminescent efficiency vs. activator concentration CaO:Pb. UV emission at room temperature. X = experimental points; curve calculated from $n = 4000$, $\alpha = 2.5 \times 10^{-4}$, $K = 7.6$.

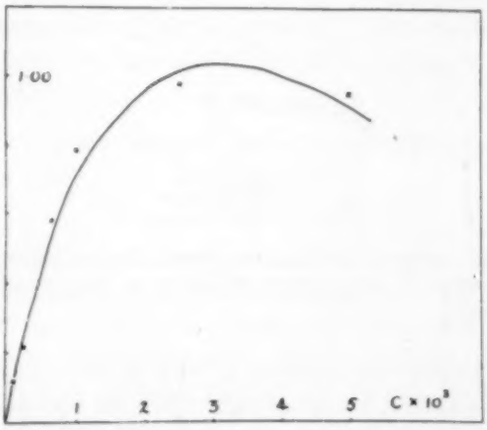

FIG. 7. Luminescent efficiency vs. activator concentration CaO:Pb. Yellow emission. X = experimental points from Fonda and Froelich; curve calculated from $n = 333$, $\alpha = 4 \times 10^{-3}$, $K = 4.75$.

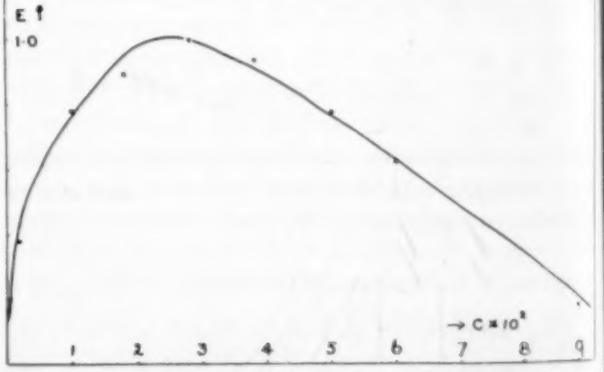

FIG. 8. Luminescent efficiency vs. activator concentration ZnF_2:Mn. Excited by x-rays. Experimental points from Johnson and Williams; curve calculated from $n = 40$, $\alpha = 0.05$, $K = 6.4$.

Comparison of Theory with Experimental Results

In Fig. 3 through 9 and in Table I calculations based on the modified theory developed earlier in this paper are compared with the experimental results obtained by the methods just described, as well as with some of those given by Johnson and Williams (3) and by Fonda and Froelich (6). It will be seen that the agreement is generally quite good except in some cases at high concentrations and for some of Johnson's and Williams' results where the experimental points do not lie on a smooth line. In Table I, the column marked "Observed" refers to the measurements of Johnson and Williams (estimated

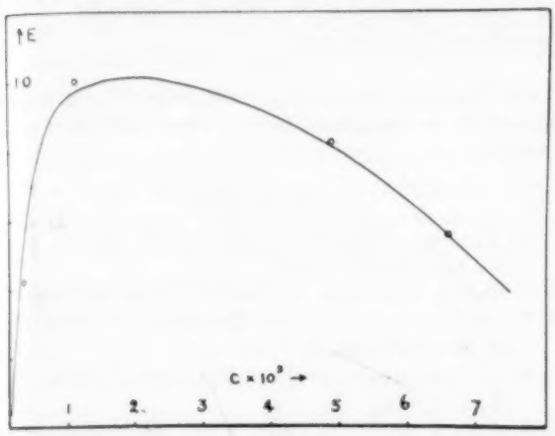

Fig. 9. Luminescent efficiency vs. activator concentration KCl:Tl. 3050 emission at −193°C; ○ = experimental points from Johnson and Williams; curve calculated from $n = 500$, $\alpha = 5 \times 10^{-4}$, $K = 1.80$.

from their graphs) and the column marked "Calculated" was obtained from the formula:

$$E = K/[1 + \alpha c^{-1} \exp nc].$$

The theory has, of course, been oversimplified.

1. No account has been taken of the fact that one type of excitation may excite more than one type of emission. For example, Hg 2537 excites the yellow as well as the ultraviolet band of CaO:Pb.

2. There will be some absorption of the excitation and emission by the nonradiative activator centers, which may become appreciable at concentrations considerably exceeding the optimum, and in cases where excitation overlaps emission.

3. Even in the purest and most carefully annealed crystal phosphor there will be a number of different competitive structure centers.

Strictly speaking, the expression for the efficiency should be of the form

$$E = \frac{K}{1 + \sum \alpha c^{-1} \exp(nc)}$$

TABLE I. *Relative efficiencies of various phosphors*

Molar concentration of activator	Relative efficiency (arbitrary units)	
	Observed	Calculated
Phosphor: ZnF_2:Mn (excited by λ 1849 Å at −193°C) $n = 13$, $\alpha = 0.24$, $K = 9.6$		
0.018	0.57	0.54
0.028	0.72	0.72
0.038	0.87	0.84
0.052	0.92	0.95
0.062	1.00	0.99
0.090	0.98	0.99
Phosphor: ZnF_2:Mn (excited by λ 1850 Å at 25°C) $n = 30$, $\alpha = 0.4$, $K = 33$		
0.0025	0.21	0.19
0.009	0.55	0.57
0.018	0.64 (this point well below smooth curve)	0.84
0.028	0.92	0.97
0.038	0.98	0.99
0.052	1.00	0.92
0.062	0.84	0.72
0.090	0.42	0.49
Phosphor: KCl:Tl (3050 emission at 25°C) $n = 550$, $\alpha = 10^{-4}$, $K = 1.5$		
0.00025	0.77	0.79
0.0011	1.00	0.99
0.0048	0.82	0.88
0.0066	0.77	0.74
Phosphor: KCl:Tl (3775 emission at −193°C) $n = 120$, $\alpha = 5 \cdot 10^{-3}$, $K = 2.5$		
0.00025	0.16	0.12
0.0011	0.37	0.40
0.0048	0.91	0.88
0.0066	0.97	0.94
Phosphor: KCl:Tl (4750 emission at −193°C) $n = 280$, $\alpha = 3 \cdot 10^{-2}$, $K = 3.3$		
0.00025	0.17	0.24
0.0011	0.72	0.70
0.0048	0.97	0.99
0.0066	0.84	0.84

where each α is a constant for each competitive center. The α in the simplified formula represents an average value.

Size of the Luminescent Center

There is now considerable evidence for and a wide acceptance of the view, originally developed by Ewles (2), of a large luminescent center. Ewles and Curry (7) found that the addition of small amounts of lead to CaO:Bi phosphors suppressed the Bi emis-

TABLE II. *The radial extent (r) of the luminescent center in terms of lattice parameter*

		n	r
Ewles & Lee	CaO:Pb (yellow emission)	250	4.0
	CaO:Pb (ditto Fonda's results)	330	4.3
	CaO:Pb (ultraviolet emission)	4,000	10.0
	CaO:Bi (low temperature band)	1,250	6.8
	CaO:Bi (high temperature band)	825	5.8
Johnson & Williams	KCl:Tl (3050 emission at 25°C)	550	5.2
	KCl:Tl (3050 emission at −193°C)	500	5.0
	KCl:Tl (3775 emission at −193°C)	120	3.1
	KCl:Tl (4750 emission)	280	4.1
	ZnF_2:Mn (excitation < 1850)	40	2.15
	ZnF_2:Mn (excitation = 1850 at 25°C)	25	1.84
	ZnF_2:Mn (excitation = 1850 at −193°C)	13	1.5
	ZnF_2:Mn (excitation 1850)	33	2.1
	ZnF_2:Mn (x-ray excitation)	40	2.15
	ZnS:Cu (Pearlman's results quoted by Johnson and Williams)	10,000	10.6

sion completely. They concluded that there must be a transfer of energy from the excited Bi center to the Pb center. For this to occur, as it did, at concentrations of lead as low as 10^{-5}, suggests the overlapping of centers having effective radii of some 5 lattice spacings.

Gibson (8) and Gibson and Garlick (9), from measurements of dielectric constants of phosphors, gave some evidence for centers which are large and complex.

Mott and Gurney (10), and Mott (11) picture a foreign ion or atom in the crystal as if in a continuum of high dielectric constant and having an associated electron moving in a large orbit embracing a considerable number of lattice ions.

Simpson (12) has calculated the charge distribution and energy levels of electrons trapped at two types of lattice defects in ionic crystals (interstitial ions and F centers). He finds that the associated wave function may spread over several lattice spacings.

In the final expression relating efficiency to concentration, developed in the present paper, an estimate of the radius of the centers may be obtained from the experimental results. For n is the number of lattice ions associated with the center and, if it is assumed that the center is spherical, then its "radius" is calculable from the value of n which is given experimentally by the optimum concentration, since $n = 1/c$ is the optimum.

The results of such calculations are given in Table II. It will be seen that the estimates are of the order expected from calculations such as those carried out by Simpson.

Any discussion of this paper will appear in a Discussion Section, to be published in the June 1954 issue of the JOURNAL.

REFERENCES

1. P. LENARD, "Handbuch der Physik," Vol. 23, p. 569, Springer, Berlin (1926).
2. J. EWLES, *Proc. Roy. Soc. London*, **A129,** 509 (1930).
3. P. D. JOHNSON AND F. E. WILLIAMS, *J. Chem. Phys.*, **18,** 323, 1477 (1950).
4. W. W. PARKINSON AND F. E. WILLIAMS, *J. Phys. Chem.*, **18,** 534 (1950).
5. J. EWLES AND C. CURRY, *Proc. Phys. Soc. London*, **A63,** 708 (1950).
6. G. R. FONDA AND H. C. FROELICH, Cornell Symposium on Solid Luminescent Materials, Paper 24, p. 385, Cornell University, Ithaca, N. Y. (1946).
7. J. EWLES AND C. CURRY, *Proc. Leeds Phil. Lit. Soc. Sci.*, **3,** 236 (1949).
8. A. F. GIBSON, Ph.D. thesis, Birmingham University, Birmingham, England (1948).
9. A. F. GIBSON AND G. F. J. GARLICK, *Proc. Phys. Soc. London*, **62,** 731 (1949).
10. N. F. MOTT AND R. W. GURNEY, "Electronic Processes in Ionic Crystals," 2nd ed., p. 84, Clarendon Press, Oxford, England (1948).
11. N. F. MOTT, *Proc. Inst. Elec. Engrs. London*, **96,** 254 (1949).
12. J. H. SIMPSON, *Proc. Roy. Soc. London*, **A197,** 269 (1949).

II. Effects of Concentration of Activator, of Temperature, and of Flux on the Excitation and Emission of CaO:Bi Phosphors

ABSTRACT

The components of the sharply resolved ultraviolet band of CaO:Bi, where peak wave lengths can be determined to ± 20 cm^{-1}, do not show any appreciable shift with concentration of activator or flux, or with temperature. The band is quenched at about 190°K and is replaced by a broad featureless band which increases in intensity up to about 570°K and then decreases. The excitation spectra of CaO:Bi show two peaks (at 2250 and 3470 Å) which show small shifts with temperatures (50 to 75 Å from −193°C to room temperature) and a large change of relative intensity (3:1 at −193°C and 1:1 at room temperature).

Introduction

In general, the luminescent spectra of impurity-activated solids are broad and featureless even at the temperature of liquid hydrogen. There are notable exceptions. The rare earths, whether in the pure state or in solution, give sometimes almost line-like spectra, which have been attributed to transitions within the incomplete shell of the rare earth ion shielded from external fields by completed outer shells. The sharply resolved spectra of certain chromium-activated crystals have been satisfactorily accounted for by transitions in the Cr^{+++} ion modified by vibrations of the crystal lattice (1). The spectra of uranyl salts have been resolved into band sequences showing vibrational frequencies attributable to the uranyl ion (2). In general, however, the luminescent spectra of most impurity-activated crystals consist of one or more broad featureless bands so that precise measurement and interpretation are difficult. The alkali earth oxides and sulfides activated by bismuth and by lead show, at low temperatures, luminescent spectra in the violet and ultraviolet which are resolved into narrow components. These have been shown by Ewles (3) to follow a band sequence of the form

$$\nu = \nu_e + (v_1 + \tfrac{1}{2})\omega_1 - (v_2 + \tfrac{1}{2})\omega_2 .$$

Ewles and Curry (4) noted that the vibrational frequency in the lower state is nearly the same for the same host for both bismuth and lead, but different for different hosts with the same activator. They suggested that this vibrational frequency is attributable to the host crystal. Whether this is correct or not, the relative simplicity and definiteness of the spectra of such phosphors, as compared with the broad indefinite bands emitted by most impurity-activated phosphors, make them exceptionally suitable for the investigation of the effects of changing activator concentration, temperature, and flux. This paper describes such investigations with CaO:Bi phosphors.

Experimental Arrangements and Results

The preparation and mounting of the phosphors and the arrangements for measuring luminescent efficiency have been described in Part I. The spectra were obtained with a Hilger Littrow type quartz spectrograph and photometered with a Cambridge microphotometer. The source of excitation was a Mercra high pressure mercury vapor lamp with the outer glass envelope removed. A clear silica flask of about 10 cm diameter filled with a solution in distilled water of 145 grams $NiSO_4 \cdot 7H_2O$ and 41.5 grams $CoSO_4 \cdot 7H_2O$ per liter served to focus the light on the phosphor and to remove all wave lengths between 3341 and 5779 Å.

Variation of Efficiency with Temperature

The luminescent efficiency was measured at intervals, as the liquid air cooling the phosphor evaporated and the temperature rose. For measurements above room temperature, the rhodium-plated mount was heated electrically. The results are shown in Fig. 1. It is seen that the curves can be analyzed in two parts. In the first part, (A), the intensity falls fairly rapidly with temperature and would presumably have reached zero at about 190°K. In the second part, (B), the intensity increases up to a maximum at about 570°K and then decreases.

Effect of Temperature Changes on Emission Spectra

The emission spectra of a sample of CaO:Bi containing a concentration of bismuth near the optimum were examined at the temperatures of liquid hydrogen, liquid nitrogen, liquid air, and finally at a succession of temperatures as the liquid air evaporated. Since evaporation was slow, the temperature as measured by a copper constantan thermocouple attached to the plate supporting the phosphor rose only a few degrees during the required 5-min exposure.

The sharpest component is that arising from the (0,0) transition. The components arising from transitions from the lowest level of the upper state are, in general, stronger than their neighbors arising from transitions from a higher level. It is particularly noted that those components arising from transitions to higher levels of the lower state, e.g., 0,3 and 1,3, disappear first as the temperature rises, while those arising from transitions from the higher levels of the upper state only appear as the temperature rises,

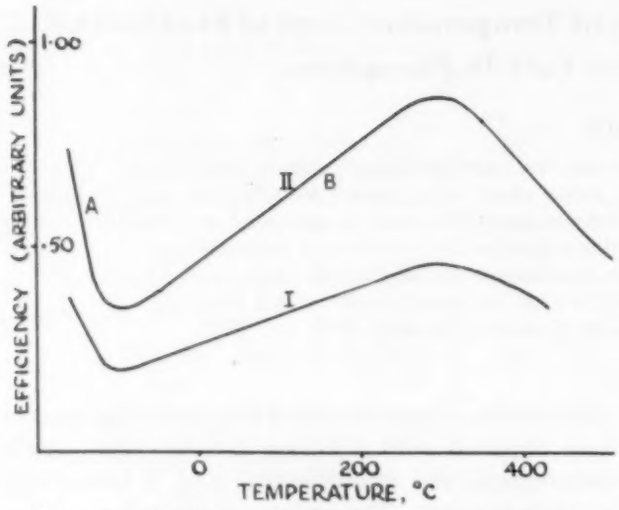

FIG. 1. Luminescent efficiency vs. temperature. CaO:Bi (5.3×10^{-4} Bi). I. No flux; II. 5% NaCl flux.

temperature band would still be much too small at the temperature at which the resolution disappears (about 190°K) to account for the broad high temperature band. It seems certain that this band is not due simply to temperature broadening of the low temperature one, but to a different process of emission. The measurements of efficiency reported in Part I suggest the existence of two centers of different radii. Whether these are of entirely separate identity or represent transitions from two different sets of energy levels of the same center cannot be determined at the moment.

Effect of Concentration of Activator on Emission Spectra

Two series of measurements have been made, one at room temperature, and the other at liquid air temperature. Photometric measurements are summarized in Tables III and IV. It is clear that there is no significant change of emission and, therefore, no change in the nature of the center with change of concentration of activator.

TABLE I. *Effect of temperature on low temperature resolved band of* CaO:Bi

$\nu = 25815 + (v_1 + \frac{1}{2})298 - (v_2 + \frac{1}{2})493$ cm^{-1}

Component	4	5	6	7	8	9	10	11	12	13
v_1	0	1	0	1	0	1	0	2	3	3
v_2	3	3	2	2	1	1	0	1	1	0
Temp, °K										
20	24250	F	24730	25030	25220	25550	25720	N	N	N
77	24230	24520	24720	25000	25210	25520	25710	N	N	N
90	24250	F	24740	F	25220	F	25720	N	N	N
99	24240	F	24730	F	25220	F	25710	N	N	N
105	24240	F	24730	F	25220	F	25710	N	N	N
125	F	N	24720	N	25200	F	25680	N	N	N
153	N	N	24750	N	25220	25500	25710	25880	26110	26600
180	N	N	24750	N	25220	25500	25710	25880	26110	26600
210	No components detected. Broad high temperature band only									

N = not detected; F = faint.

e.g., 2,1; 3,1; and 3,0. These changes of intensity distribution indicate an increasing probability of transition from higher levels of the upper state and a decreasing probability of transition to the upper levels of the lower state as the temperature rises. Within the limits of measurement (about 1 or 2 Å) there is no change of wave length with increasing temperature. Measurements of the half-widths of the components were also made as the temperature rose.

Above about 125°K, the widths of the components cannot be measured against the background of the developing broad, featureless high temperature band which is in fact present at all temperatures (see Fig. 2). The relative amplitudes of the two bands are indicated quite clearly in the figure.

It is clear from all these temperature effects that the low temperature and high temperature bands [corresponding to the parts (A) and (B) in Fig. 1] are, in fact, quite different emissions. By extrapolation, the half-widths of the components of the low

TABLE II. *Half widths of components of* CaO:Bi *low temperature band (in cms^{-1})*

Temp, °K	Component (v_1, v_2)			
	0,3	0,2	0,1	0,0
20	112	94	73	31
77	115	118	80	35
90	120	114	88	41
99	125	118	95	50
125	—	120	102	68

Effect of Flux

A series of phosphors was prepared, with a fixed concentration of activator near the optimum and varying amounts of NaCl as flux. The emission

spectra were taken at room and at liquid air temperatures. The photometric measurements on these spectra are given in Tables V and VI.

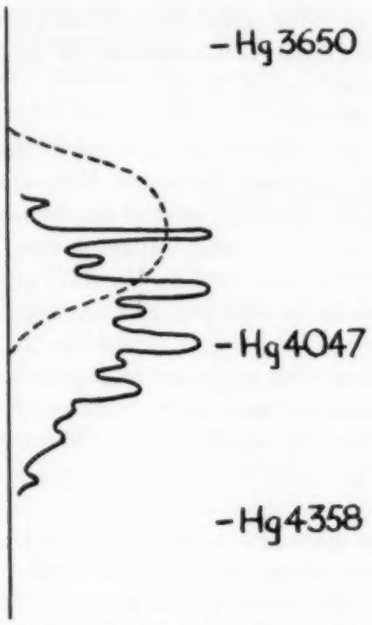

FIG. 2. Emission spectra of CaO:Bi; --- high temperature band; —— low temperature band.

Effect of variation of activator concentration on emission spectra of CaO:Bi

TABLE III. *Room temperature emission*

Concentration of Bi (atomic)	Peak wave length in Å
4.27×10^{-3}	3775
5.3×10^{-4}	3755
2.6×10^{-5}	3765

TABLE IV. *Low temperature emission (peak wave lengths in* Å)

Component	Concentration of Bi (atomic)		
	2.6×10^{-5}	5.3×10^{-4}	4.27×10^{-3}
1 ?	—	4280	4287
2 (0,4)	—	4209	4202
3 (1,4)	—	4159	4159
4 (0,3)	4121	4116	4116
5 (1,3)	—	4074	4070
6 (0,2)	4044	4045	4041
7 (1,2)	—	3994	3988
8 (0,1)	3965	3957	3955
9 (1,1)	—	3911	3912
10 (0,0)	3891	3884	3884

There is no appreciable change of wave lengths with varying flux concentration. It is concluded that the flux forms no part of the center but only promotes its formation. The effect of the flux concentration on the efficiency was also investigated at room

Effect of flux on CaO:Bi *emission*

TABLE V. *Room temperature emission*

Conc. of flux	Peak wave length in Å
%	
Nil	3775
0.2	3780
10	3770

TABLE VI. *Low temperature resolved band (peak wave lengths in* Å)

Component	Conc. of flux		
	Nil	% 0.2	% 10
1	4280	—	—
2	4209	4209	4202
3	—	—	—
4	4115	4125	4120
5	4074	4078	4071
6	4045	4043	4040
7	3994	3997	3992
8	3957	3963	3957
9	3911	3918	3911
10	3884	3888	3886

TABLE VII. *Excitation peaks of* CaO:Bi *phosphors*

Conc. of activator	Flux	Temp	Peak wave length in Å	
2.6×10^{-5}	None	Room	2300	3475
		Liq. air	2250	—
5.3×10^{-4}	None	Room	2250	3475
		Liq. air	2250	3400
5.3×10^{-4}	15% NaCl	Room	2250	3475
		Liq. air	2300	3400
4.27×10^{-3}	None	Room	2250	3450
		Liq. air	2300	3400

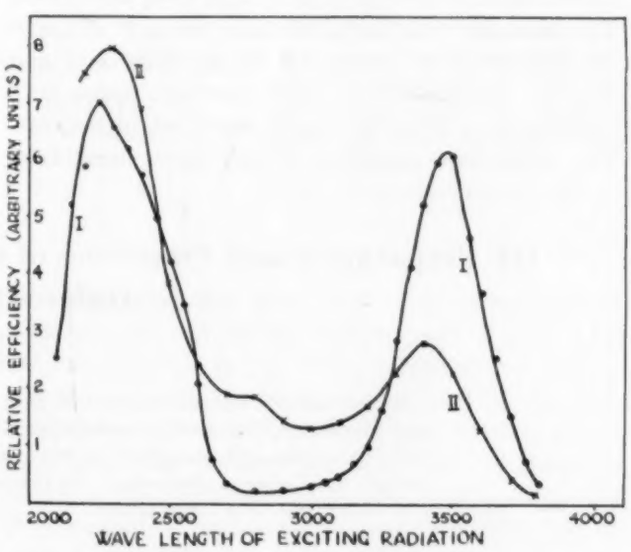

FIG. 3. Excitation spectra of CaO:Bi (5.3×10^{-4} Bi, 5% NaCl). I. At room temperature; II. at −193°C.

and at liquid air temperatures, with the arrangements described in Part I. There is an optimum efficiency at about 5 per cent flux at both liquid air and at room temperature.

Phosphorescence

To obtain the phosphorescence spectrum, the source was lined up so that the exciting light was incident on the phosphor in a direction at right angles to the axis of the spectrograph. The phosphor on its supporting plate was located on the axis of a rotating cylinder carrying sectors which eclipsed source and spectrograph slit alternately. Thus, when exciting radiation was falling on the phosphor, the slit was eclipsed and, when the slit path was open, the source was eclipsed. Any overlap would have been seen by the appearance of Hg lines, since no filters were used. At liquid air temperatures, an exposure of 3 hours with a slit width of 0.05 mm gave a picture satisfactory for photometry, but at room temperature a blank plate was obtained after an exposure of 6 hours with a slit width of 0.2 mm. Thus the phosphorescence is very temperature-dependent and is indeed obviously associated with the low temperature emission. Its spectrum is in fact identical with the resolved low temperature band.

Excitation Spectra

The variation of quantum efficiency with wave length of excitation has been measured by the method of photoelectric fluorescent photometry described recently (5). A d-c hydrogen arc supplied by a stabilized 200 volt (d-c) 500 ma power pack, provided a continuous spectrum of ultraviolet. The exciting beam was chopped at 1000 cps by a rotating slotted disk driven by a synchronous motor. It was focused on the slit of a Hilger D246 monochromator. The phosphor was mounted near the exit slit and the luminescence picked up by an Electrical and Musical Industries Ltd. 5060 photomultiplier provided with a filter to reject scattered ultraviolet. The signal was amplified further by a three-stage resistance capacitor amplifier with a parallel T network tuned to 1000 cps and the output fed to an oscilloscope for monitoring and to an a-c voltmeter for measuring.

Results of these measurements on CaO:Bi phosphors of different concentration of activator and flux are shown in Fig. 3.

It is noted that:

1. The flux causes no significant change, confirming the previous deduction from the emission spectra that it forms no part of the center.

2. The shift with temperature is very small, but the ratio of the 2250 peak to the 3475 peak changes from approximate equality at room temperature to 3/1 at the temperature of liquid air. It is certain, however, that both peaks are able to excite both the low temperature and high temperature emission bands so that the significance of this change in the excitation spectrum is not at all clear.

3. Highly purified nonluminescent calcium oxide prepared as described in Part I showed no excitation peaks in the range of excitation studied (2000 to 3900 Å) so that the excitation peaks of the phosphor are due to direct excitation at the centers.

The results of all these investigations are discussed, in conjunction with those described in Parts I and III, at the end of Part III.

Any discussion of this paper will appear in a Discussion Section, to be published in the June 1954 issue of the JOURNAL.

REFERENCES

1. O. DEUTSCHBEIN, *Ann. Phys.*, **14,** 7 (1932).
2. S. H. DIEKE AND A. B. F. DUNCAN, "Spectroscopic Studies of Uranium," National Nuclear Energy Series III, **2,** p. 41, McGraw Hill Book Co., Inc., New York (1949).
3. J. EWLES, *Proc. Roy. Soc. London*, **A129,** 509 (1930).
4. J. EWLES AND C. CURRY, *Proc. Phys. Soc.*, **A63,** 708 (1950).
5. J. EWLES, *Proc. Leeds Phil. Lit. Soc. Sci. Sect.*, **5** [3], 236 (1949); J. EWLES AND C. N. HEAP, *Trans. Faraday Soc.*, **48,** 331 (1952).

III. Preparation and Properties of Calcium Oxide Phosphors with Eleven Different Activators

ABSTRACT

Preparation of the phosphors and their emission and excitation spectra are described and discussed. The need for a reducing atmosphere in the case of some activators and the production of a phosphor by heating very pure CaO in vacuo are noted and discussed. In a general discussion, the results reported in the three papers are related to the conception of a large center.

INTRODUCTION

Although it has been well known for a long time that calcium oxide can be activated by a considerable number of different metals, the phosphors produced are not, in general, of high efficiency and have not so far aroused much interest. A comparison of

the effects of different activators in a host of such simple crystal structure and of good thermal and chemical stability should, however, provide useful data for the theory of luminescence and of the solid state. This paper describes some experiments which have recently been carried out in this field. An attempt is made to draw some general conclusions from the results taken in conjunction with those reported in Parts I and II.

TABLE I. *Calcium oxide phosphors; effect of firing atmosphere*

Activator (conc. by weight)	Heat-treatment	Visible luminescence
Sb (10^{-3})	In air, 650°C, ¾ hr	Poor
Sb (10^{-3})	In H_2, 650°C, ¾ hr	Bright yellow green
Sb (3%)	H_2, 650°C, ¾ hr	Dead, discolored
Bi (1.2×10^{-3})	Air, 650°C, 20 min	Bright violet
Bi (1.2×10^{-3})	H_2, 650°C, 20 min	Poor, discolored
Bi (2×10^{-4})	H_2, 620°C, 1 hr	Bright violet
Cu (10^{-3})	H_2, 650°C, 20 min	Bright green
Cu (10^{-3})	Air, 650°C, 20 min and many other times and temperatures	Very dull
Mn (10^{-3})	H_2, 650°C, ½ hr	Strong red
Mn (10^{-3})	Air, 650°C, ½ hr	Very dull
U (10^{-3})	H_2, 600°C, ¾ hr	Bright greenish yellow
U (8×10^{-4})	Air, 600°C, ¾ hr	Bright greenish yellow
Pb (10^{-3})	H_2, 600°C, 20 min	Bright white
Pb (10^{-3})	Air, 600°C, 20 min	Bright yellow
Pb (10^{-4} to 10^{-6})	Air or H, 600°C, 20 min or longer	U.V. only
Ti (2×10^{-3})	Air, 500°C, ¾ hr	Bluish white, moderate
Sn (5×10^{-4})	H_2, 700°C, 40 min	Bright bluish white
Sn (7×10^{-4})	Air, 700°C, 40 min	Weak bluish
Tl (2×10^{-4})	Air, 500°C, ½ hr	Bright yellow
Mo (2×10^{-3})	Air, 500°C, ¾ hr	Whitish, moderate
As (10^{-3})	H_2, 700°C, ½ hr	Yellow, fairly good
As (10^{-3})	Air, 700°C, ½ hr and other times and temperatures	Poor

Experimental

Preparation of the Phosphors

The preparation of highly purified calcium oxide showing no appreciable luminescent efficiency after firing in air, and the treatment required to produce good phosphors activated with bismuth have been described in Part I. With some other activators (Pb, U, Tl, Ti) similar firing in air gave good phosphors. With still others, while firing in hydrogen gave good results, firing in air gave very low efficiency. The need for a reducing atmosphere suggests the possibility that in such cases the metal is only effective in a lower valency state. A sample containing a concentration of bismuth which gives the optimum on firing in air gave, when fired in hydrogen, a discolored product of very low efficiency. Similar results were obtained in other cases, suggesting that, at least in some cases, the activator must be in an ionic state and the reduction to the metallic state renders it inoperative as an activator. Some results are summarized in Table I.

Calcium oxide heated in vacuo.—A sample of pure calcium oxide was placed in a platinum boat in a nonluminescent silica tube connected to a vacuum system, and heated in an electric furnace under a vacuum of 10^{-5} mm Hg. The samples were examined under ultraviolet ($\lambda < 3341$) after varying heat-treatment. The observations are collected in Table II.

Heating in air removed the discoloration of samples IIb and III and further heating in vacuo for 1 hour at 1000°C again gave bright luminescent products.

TABLE II. *Calcium oxide heated in vacuo*

Sample	Time of heating	Temp, °C	Luminescence
Ia	30 min	900	Faint
Ib	Further 1 hr	900	Appreciable blue white luminescence
IIa	1 hr	1000	Bright blue luminescence
IIb	3 hr	1000	Nonluminescent discolored gray
III	3 hr	1250	Nonluminescent discolored gray

It is suggested that here, as in other cases reported from this laboratory, the luminescence produced by heating in vacuo is due to the production of vacant oxygen sites. This is being investigated further. Assuming that the concentration of anion defects necessary to give appreciable luminescence is of the same order as that for foreign ions, estimates based on the free energy of oxides (1) indicate that the partial reduction to be expected under the conditions employed is quite sufficient to provide such concentrations. Since the lattice would have an excess of posi-

TABLE III. *Emission peaks of* CaO *phosphors*

Activator	Type of photo plate (Kodak) or photo-multiplier (P/M)	Temp	Wave lengths of peaks			
Cu	OD	Room	4725	5450	—	
	P/M	Room	4800	—	—	
	OD	Liquid air	4775	5450	6150	
Sb	OD	Room	4900	5580	6100	(?)
	P/M	Room	4900	—	—	
	OD	Liquid air	—	5525	5900	(?)
Sn (prepd. in air)	OD	Room	4500	5200		
	P/M	Room	4750	5300		
	OD	Liquid air	4725	5500	6050	
Sn (prepd. in H_2)	OD	Room	4600	5350		
	OD	Liquid air	4750	5450	6050	
Tl	OF	Room			5920	
	OF	Liquid air			5800	6500
Mo	OF	Room	4650		5800	
	P/M	Room	4720			
	OF	Liquid air	4775		5900	
Ti	OF	Room	4800			
	P/M	Room	4850			
	OF	Liquid air	4650		5875	
Mn	OF	Room			6080	
Pb (in H_2)	OF	Room	3650		6000	6400
	OF	Liquid air	3650 (resolved)		6000	6400
As	OD	Liquid air	5600		6150	

TABLE IV. CaO:U

Component	Intensity	Wave length	Wave no.	Calc.*	n_1	n_2
1	Strong	5555	18002	18002	0	0
2	Weak	5650	17700	17698	1	1
3	Strong	5765	17346	17342	0	1
4	Weak	5865	17050	17036	1	2
5	Strong	5995	16680	16680	0	2

* Calculated from the band formula $\nu = 18157 + (v_1 + \frac{1}{2})356 - (v_2 + \frac{1}{2})662$ cm^{-1}.

tive charge if the free oxygen ions left as such, it is supposed that they first combine to give O_2 molecules, leaving electrons which are then trapped at the vacant oxygen sites, forming F centers which are luminescent. The discoloration produced by long heating in vacuo at high temperatures is then attributable to the development of an F center absorption in the visible, an effect well known in the case of alkali halides and zinc oxide. The peak of luminescent emission is at about 3800 Å and the

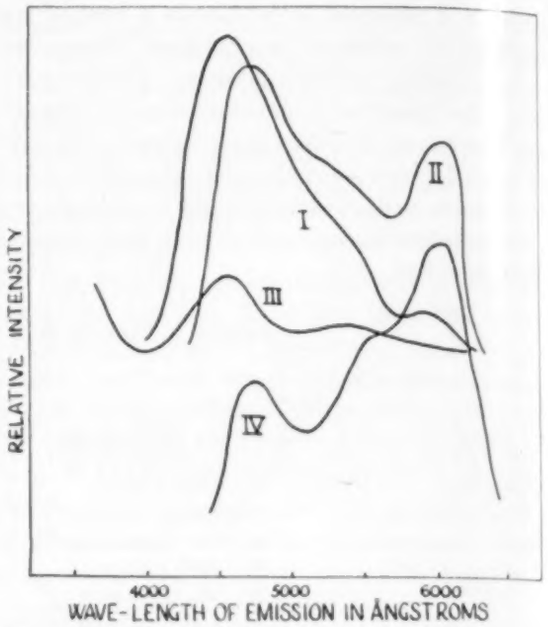

FIG. 1. Emission spectra of CaO:Sn. Curve I, prepared in H_2, emission at 20°C; curve II, prepared in H_2, emission at −193°C; curve III, prepared in air, emission at 20°C; curve IV, prepared in air, emission at −193°C.

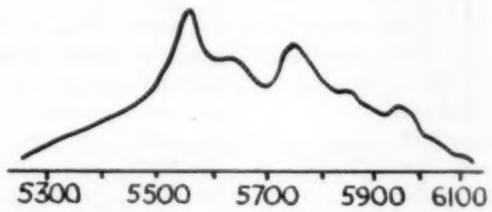

FIG. 2. Emission spectra of CaO:U at −193°C

TABLE V. *Excitation spectra of* CaO *phosphors*

Activator	Wave lengths of excitation peaks in Å
Sb	2700
Cu	2300
Pb (8×10^{-3})	2800 3375
Pb (1.35×10^{-4})	2400 2800
Pb (in H_2)	2450
Sn (prepd. in H_2)	3150 (3500) and rising toward shorter wave lengths (2000 Å)
Sn (prepd. in air)	3200 (3500) and increasing at 2200 Å toward shorter wave lengths
Mo	2500 2700
Ti	2300 3000 (the 3000 Å is a very broad peak)
Tl	3300 and increasing at 2200 Å toward shorter wave lengths
U (heated in air)	2200
U (heated in H_2)	2200
Bi (heated in air)	2250 3475
Bi (heated in H_2)	2250 3475
As	2200

The excitation peaks have a half-width of the order of 200 Å.

Pure CaO has no excitation peak in the range 2000 to 3900 Å.

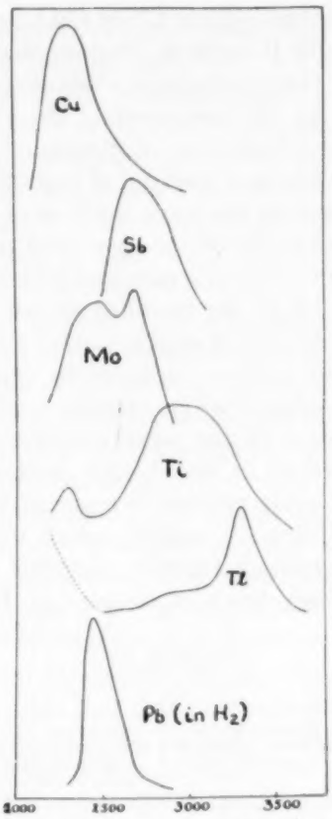

FIG. 3. Excitation spectra of CaO phosphors with different activators.

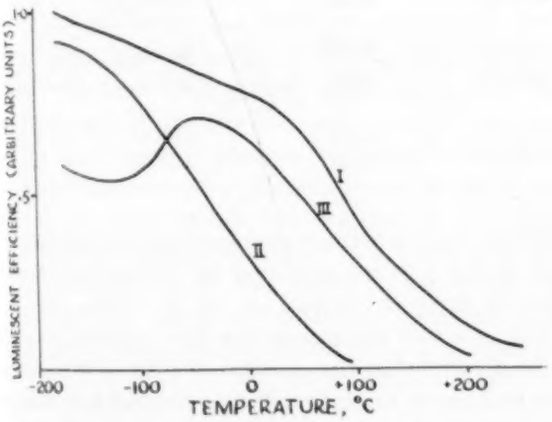

FIG. 4. Dependence of luminescent efficiency on temperature. Curve I, CaO:Tl; curve II, CaO:U; curve III, CaO:Sn (prepared in H_2).

half-width of the band is about 1 ev, i.e., wider than the usual bands introduced by foreign ion activators (e.g., see next section).

Emission Spectra

The luminescent emission spectra were obtained as described in Part II. Some measurements were also made photoelectrically with arrangements similar to those described in Part II. The phosphor was placed before the entrance slit of the monochromator and excited by a chopped beam from a mercury vapor

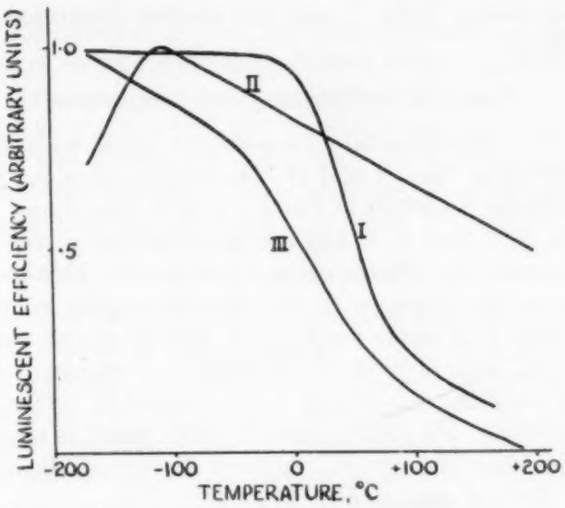

FIG. 5. Dependence of luminescent efficiency on temperature. Curve I, CaO:Pb, yellow emission, 3650 Å excitation; curve II, CaO:Pb, u.v. emission, 2537 Å excitation; curve III, CaO:Ti.

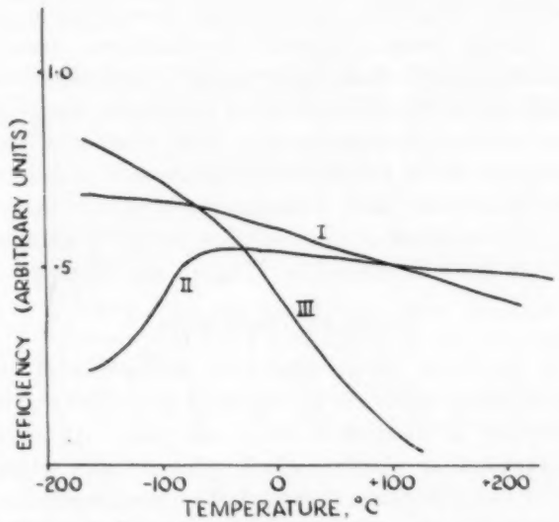

FIG. 6. Dependence of luminescent efficiency on temperature. Curve I, CaO:Cu; curve II, CaO:Sb; curve III, CaO:Mo.

lamp filtered through a Bowen filter. The signal was picked up by a photomultiplier behind the exit slit and amplified and detected as described in Part II. The peaks of the bands are given in Tables III and IV and some photometer curves in Fig. 1 and 2. The vibrational frequency 662 cm^{-1} shown by the CaO:U band in the lower state does not agree with that shown by the resolved bands in CaO:Pb and CaO:Bi reported earlier (2) and attributed to a vibration of the CaO lattice. It may be that the 662 cm^{-1} frequency shown by CaO:U is associated with the complex O—U—O.

Excitation Spectra

The photoelectric method described in Part I was used. The peak wave lengths of excitation are sum-

marized in Table V and the spectra illustrated in Fig. 3.

Variation of Efficiency with Temperature

The experimental arrangements have been described in Parts I and II. The results, obtained by methods described in Parts I and II, are shown in Fig. 4, 5, and 6. It has not been possible as yet to separate the effects of multiple bands. However, where the response of the photomultiplier is due mainly to a single band either because of the wave length sensitivity of the instrument or through the nature of the emission, as in the cases of Pb (yellow), Ti (4850), Mo (4650), and Tl (5800–5900), it would seem that the curves approach a course indicated by the law suggested by Mott (3):

$$E = 1/[1 + Ae^{-W/kT}]$$

where W is the energy required to produce a transition from the excited state to one from which a nonradiative transition can be made to a lower state, the energy being dissipated in vibrational quanta. The conception of the large center would afford the possibility of the dissipation of excitation energy by simultaneous distribution of a large number of phonons over the large number of lattice cells associated with the center. Such a dissipation of optical quanta in a large number of relatively low energy quanta has already been suggested by Möglich and Rompe (4).

General Discussion

It has been shown that the conception of the luminescent center (in an impurity-activated crystal phosphor) as an atom or ion of activator with which is associated an electron whose orbit includes a large and definite number of host lattice ions, leads to a relation between efficiency and concentration which is in good accord with experimental results. The sharpness of the levels involved in the low temperature resolved bands of CaO:Bi and CaO:Pb (2) and the small effect of changes of temperature, concentration, or flux on the width and positions of these sharp levels and on the excitation and emission peaks of CaO activated by various metals, also suggest a definite configuration for the centers. It would seem reasonable to expect that the actual configuration should depend on both host crystal and on activator. Indeed there can be no question that the nature of the host crystal affects the nature and size of the center with the same activator (2, 5). The effect of quenching or annealing is well known and the effect of structure defects on efficiency has been discussed in the theory of efficiency developed in Part I. The implications for the preparation of phosphors are obvious. The precision measurements on the resolved bands of CaO:Bi reported in Part II and by Ewles and Curry (2) on CaO, SrO, and MgO activated with Bi or with Pb show that, at least in these cases, the centers have a vibrational frequency determined by the host crystal. The ideas of Mott (6) and the calculations of Simpson (7) regarding the host crystal as a medium of high dielectric constant determining the wave function of the electron associated with the center have been referred to in Part I. There it was also seen that an estimate of the "radius" based on the modified theory of efficiency gives results for center sizes in CaO of the same order of magnitude as those obtained by Simpson for F centers and interstitial ion centers in alkali halides. An examination of the wave numbers of the electronic transitions in the sharply resolved bands of alkali earth oxide phosphors reported here and by Ewles and Curry (2) suggest indeed the possibility of a simple relation between dielectric constant of host and energy levels of center (see Table VI).

TABLE VI

Phosphor	Wave number of electronic transition in resolved band	Dielectric constant of host crystal calculated from refractive index at emission wave length (K)	$\nu \cdot K \times 10^{-4}$
	ν in cm^{-1}		
MgO:Bi	28460	3.110	8.86
CaO:Bi	25815	3.565	9.15
SrO:Bi	24180	3.680	8.90
CaO:Pb	27526	3.565	9.77
SrO:Pb	26538	3.680	9.75
MgO:U	20855	3.014	6.28
CaO:U	18002	3.379	6.08

These results seem to imply that the emission is that of the free ion modified by the dielectric constant of the host crystal, i.e., $\nu_{cryst.} = \nu_{vac.}/K$.

The effect of changes in the host crystal is again to be discerned in the changes of intensity distribution and loss of resolution of the resolved low temperature band of CaO:Bi and in the mixed phosphors CaO·SrO:Bi. Ewles and Curry (2) reported that the addition of SrO to CaO:Bi results in the progressive loss of resolution up to a Sr/Ca ratio of 1/4, when resolution is entirely lost, reappearing again with the vibration frequency characteristic of SrO at 90 per cent Sr. Now, assuming Vegard's law and taking the lattice constants of CaO and SrO as 4.80 and 5.15 Å, this corresponds to disappearance of resolution at a fractional expansion of the CaO lattice of about 1.6 per cent. It was shown in Part II that the resolved band of CaO:Bi disappeared at about 190°K after no serious broadening or shift of frequencies. From measurements of the thermal expansion of BaO and SrO by x-ray diffraction re-

ported by Eisenstein (8), and with a reasonable extrapolation, the thermal expansion of CaO from absolute zero to 200°K is about 1.2 per cent which is of the same order as the lattice distortion leading to disappearance of resolution in SrO·CaO:Bi.

The change in intensity distribution with temperature among the components of the resolved band, and the change of peak wave length of excitation with temperature may be explained by a change with lattice expansion of the potential energy curves of the upper and lower states involved in the excitation and emission processes. The experimental evidence that the centers produced by different activators in the same host are entirely specific to each activator does not appear to be quite conclusive. The resolved emission bands of CaO:Bi and CaO:Pb do indeed appear to be different, but even here the (0-0) transitions are quite close—3887 Å for Bi and 3650 Å for Pb. The colors, efficiencies, and variations of efficiency with temperature in the phosphors of CaO activated with Bi, Pb, Ti, Cu, Sb, Sn, Mo, Tl, Mn, U, and As are quite different, and at first sight the emission and excitation spectra seem to be specific to each activator. However, an examination of the emission spectra (Table III) shows that there are bands whose peaks are not very different with different activators, e.g., Cu 4725, Sb 4900, Sn 4600, Mo 4650, Ti 4800, and in the red Cu 6150, Sn 6050, Mo 5990, Mn 6080, Pb 6000. Thus, although the evidence is somewhat in favor of the view that each activator forms a specific and characteristic center, it does not exclude the possibility that the activator merely provides an ion of suitable valency and polarizability with which the electron responsible for luminescence is associated in a way that depends on the host crystal and, only to a limited extent, on the actual nature of the ion. Rothschild (9) has given evidence from ZnS phosphors which supports the latter view. The existence of multiple bands with the same activator is most simply explained by the existence of more than one excited level for the large center envisaged here. This view is in accord with those of Kroeger and Zalm (10) and of Wise (11), and with the different radii estimated from the theory of efficiency for different bands with the same activator (Part I, Table I).

Acknowledgments

The authors wish to acknowledge their gratitude to Professor R. Whiddington, C.B.E., F.R.S., for his interest in the work and for the facilities afforded them in the Department of Physics of The University of Leeds. One of the authors (J. E.) is indebted to the Leverhulme Foundation for a Research Fellowship whose tenure extended over part of the period of the work, and the other (N. L.) to the Board of Education and to The University of Leeds for personal grants. Some of the apparatus used was purchased from a Grant from the Government Grant Committee of The Royal Society.

Any discussion of this paper will appear in a Discussion Section, to be published in the June 1954 issue of the Journal.

References

1. H. J. T. Ellingham, *J. Soc. Chem. Ind. London*, **63**, 125 (1944).
2. J. Ewles and C. Curry, *Proc. Phys. Soc. London*, **A63**, 708 (1950).
3. N. F. Mott, *Proc. Roy. Soc. London*, **167A**, 384 (1938).
4. F. Möglich and R. Rompe, *Z. Physik*, **115**, 707 (1940); **117**, 119 (1940).
5. J. Ewles, *Proc. Roy. Soc. London*, **129A**, 509 (1930).
6. N. F. Mott, *Proc. Inst. Elec. Eng. London*, **96**, 254 (1949).
7. J. H. Simpson, *Proc. Roy. Soc. London*, **197A**, 269 (1949).
8. A. Eisenstein, *J. Appl. Phys.*, **17**, 443 (1946).
9. S. Rothschild, *Trans. Faraday Soc.*, **42**, 640 (1946).
10. F. A. Kroeger and P. Zalm, *J. Electrochem. Soc.*, **98**, 177 (1951).
11. M. E. Wise, *Physica*, **17**, 1011 (1951).

Attempts at the Electrolytic Initiation of Polymerization[1]

H. Z. Friedlander,[2] Sherlock Swann, Jr., and C. S. Marvel

The Chemical Laboratories of the University of Illinois, Urbana, Illinois

ABSTRACT

Four cathodic and four anodic reactions which should produce free radicals were carried out in the presence of a vinyl monomer under a wide variety of conditions. The cathodic reactions studied were the reduction of acetophenone and the discharge of methyl, benzylquinolinium, and *p*-bromobenzenediazonium ions. The reactions of the following anions were investigated: laurate, *p*-benzyl phenolate, hydroxyl, and tricarboethoxylmethyl. The various classes of emulsifiers were used, namely cationic, anionic, neutral ionic, and nonionic. The intermediates formed at the electrodes did not react with the monomers. A reinvestigation of the electrolytic reduction of acetophenone in acid solution is also reported.

Introduction

It has recently been shown that polymerization of vinyl monomers may be initiated by electrolytic reduction (1) and by the electrolytic regeneration of a reducing activator (2). Although an attempt to initiate polymerization by means of the Kolbe synthesis (2) failed, the electrolytic method offered so many other possibilities that it seemed worthy of further investigation. It was, therefore, decided to study several anodic and cathodic reactions.

The components and proportions of standard formulations for polymerization were used as electrolytes except for the substitution of a depolarizer for the usual chemical initiator. Both ionizable and nonionizable compounds served as free radical sources at the electrodes. The following cathodic reactions were studied: the reduction of acetophenone (5), and the discharge of methyl (6), quaternary quinolinium (7), and diazonium (8) ions. The behavior of the anodic products from the electrolysis of the following ions was studied: laurate, tricarboethoxymethyl (9), a phenolate (10), and hydroxyl.

Acetophenone was the only depolarizer used which in itself, without a monomer, leads to a polymeric material.

Discussion of Results

Cathodic Reactions

To begin the investigation it was decided to restudy the reduction of acetophenone in acid solution carried out previously in these laboratories (5). It had been found that a resinous material was formed in the reaction as well as the pinacol, suggesting a free radical, $ArC(CH_3)OH$ as an intermediate in the reduction. Since the formation of the pinacol was assumed to be a free radical terminating reaction, a study was made to find out at which cathode the least pinacol formation occurred. The electrolysis was carried out in the same manner as in the earlier study (5) except for the use of cast electrodes of 99.95 per cent purity rather than commercial grade sticks of the metals (platinum excluded). The method for the recovery of the products also differed somewhat from that previously used. At the conclusion of the run, the ether soluble fraction was boiled in hexane ("Skellysolve B"), and then chilled slowly, first to 0° and then to the temperature of a dry ice-acetone mixture. The crystals which separated were those of the high-melting form of the pinacol. These were crystallized from hexane ("Skellysolve B"); mp 120–121°C. The results are shown in Table I.

Approximately double the amounts of the normal high-melting form of the pinacol reported in the previous study (5) were isolated. By fractionation with an 8-in. column packed with glass helices at a pressure of 0.4 to 0.5 mm of mercury the high boiling liquid product which had not crystallized was separated into three fractions, a liquid, a liquid resin, and amorphous solid. The boiling ranges were 125°–138°C, 155°–180°C, and 200°–210°C, respectively. After standing at room temperature for several hours, crystals spontaneously precipitated from the first and second fraction. The melting point of about 82°C and the analyses indicated that the crystalline material was probably rich in the low-melting form

[1] Manuscript received December 15, 1952. This paper was prepared for delivery before the New York Meeting, April 12 to 16, 1953. This research was carried out under the sponsorship of the Reconstruction Finance Corporation, Synthetic Rubber Division. It is taken from part of the doctoral dissertation of Henry Z. Friedlander submitted to the Graduate College of the University of Illinois.

[2] Present address: American Cyanamid Company, Stamford, Connecticut.

of the pinacol. The exact melting point varied with different samples and the low-melting isomer (82°C) changed to the high melting (120°–121°C) on repeated crystallizations.

Calculated C, 79.33; H, 7.43.

Found C, 79.33; H, 7.56.

These fractions had been previously reported as consisting of bis-(α-methyl)benzyl ether. It might be mentioned that bismuth had not been tried as a cathode for this reduction before. It was used in the attempts at polymerization on account of its comparative inactivity in the formation of pinacol.

The reduction of acetophenone was performed repeatedly in the presence of styrene and acrylonitrile. Conditions favorable to two types of polymerization, solution in an acid-alcohol-water catholyte, and emulsion by cationic, anionic, neutral ionic, and nonionic agents, were studied. Limited polymerization did take place, but in these instances the presence of acetophenone was not vital, showing that the reaction was merely a repetition of the work of Wilson (1). An important point is the necessity for total emulsification. If emulsification were not complete, even a nonelectrolytic system containing benzoyl peroxide did not initiate polymerization.

The free radicals generated by the electrolysis of quaternary pyridinium and quinolinium salts seemed suitable since the intermediate involved in the formation of dihydrobipyridines and dihydrobiquinolines (7) is resonance stabilized.

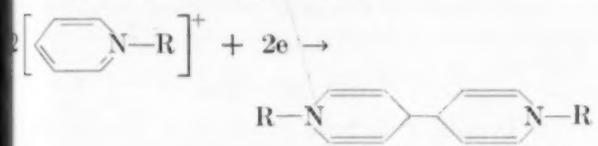

For more efficient contact with the monomer, the free radical should be soluble in the organic phase of an emulsion. For this reason, salts of high molecular weight such as benzylquinolinium chloride were used with potassium laurate as the emulsifier. Tarry material formed at the cathode, which was of smooth platinum, but not polymer.

In a similar manner, the electrolysis of *p*-bromobenzenediazonium fluoborate caused no polymerization of acrylonitrile. The fluoborate ion was chosen to insure stability of the diazonium ion during electrolysis. A smooth platinum cathode was used in the hope of avoiding reduction to the phenylhydrazine. Also, the electrolysis of methyl iodide under the same conditions failed to initiate the polymerization of styrene.

Anodic Reactions

The first anodic reaction studied was the electrolytic discharge of the tricarboethoxymethyl ion (12).

$$2 - C(COOC_2H_5)_3 \rightarrow (C_2H_5OOC)_3CC(COOC_2H_5)_2$$

The usual pink-white coupled product (mp 103°–103.5°C) formed on the anode during repeated electrolyses in the presence of styrene emulsions and suspensions. Even the use of equimolecular amounts of styrene and the ester led to no addition compound or polymer. In these experiments the formation of hexacarboethoxyethane caused partial insulation of the anode after four hours.

TABLE I. *A study of cathode materials for the reduction of acetophenone in acidic solution*

Anode: lead; anolyte: 10 per cent sulfuric acid; cathodic area: 100 cm²; catholyte: 80 ml of a mixture of 250 ml water, 550 ml ethanol, and 300 g sulfuric acid, containing 20 g of acetophenone. Duration of run approximately theoretical for reduction of ketone to hydrocarbon; temperature: 62°–67°C.

Run no.	Cathode	Grams of recrystallized pinacol, high-melting form	Current (amp)	Current density amp/cm²	Duration of run (hours)
16A, 26	Aluminum	1.3	5.4	0.054	3
6, 7, 17	Cadmium	2.9	5.4	0.054	3¾
8, 9	Cadmium	2.2	2.5	0.025	7½
10,* 11*	Cadmium	2.7	5.4	0.054	4
12, 13, 18	Bismuth	1.4	5.4	0.054	3½
14, 15	Tin	1.5	5.4	0.054	3½

* These runs contained 0.06 g of dodecyl mercaptan in the catholyte.

Another system studied was the electrolysis of potassium laurate at lead and lead oxide anodes, conditions unfavorable for the Kolbe synthesis. In this study, potassium laurate served as a conductant, emulsifier, and source of free radicals. On two occasions, minute amounts of polystyrene and polyacrylonitrile were formed during the electrolysis, but the results were not reproducible. During the runs, a film of lead laurate formed on the anode.

Analogous electrolyses were performed with sodium *p*-benzylphenolate and sodium hydroxide alone. Again the intermediate failed to react with the monomer.

It is possible that the reactions involving organic free radicals would be successful in nonaqueous media under strictly anhydrous conditions as shown in a very recent paper (11).

Conclusions

In the reduction of acetophenone in acid and in the electrolysis of potassium triethylmethanetricarboxylate, the normal reactions proceeded regardless of the presence of monomer. It is assumed that the other reactions studied behave similarly. It would seem, therefore, that any free radical formed

did not leave the surface of the electrode to meet the monomer before undergoing a secondary reaction or that proper contact between radical and monomer on the electrode surface was never made.

Experimental

The apparatus and procedures were based on those previously reported from this laboratory (5, 12). The electrolyte in an undivided cell consisted of aqueous suspension of monomer, emulsifier, and the organic compound which was the source of free radicals. In the experiments with a divided cell, the above mixture, after the addition of sulfuric acid and, in some experiments, of 10 per cent by weight of ethyl alcohol as a blending agent, served as the catholyte. The anolyte was a 10 per cent sulfuric acid solution. The current was usually of the order of 0.3 amp. The duration of the electrolyses varied from 3 to 20 hours depending on the reaction. A low current density would provide a catalytic amount of free radical and hence would favor a high degree of polymerization. Emulsification with water lowers the energy of activation for polymerization and prevents local overheating during polymerization. Stirring, either by a blade or magnetic device, and deaeration by nitrogen bubbling through the electrolyte were used because they favor reaction of an intermediate with the monomer.

It was not known whether the presence of a charged emulsifier at the electrode where the free radical was formed would be beneficial or not. For this reason, dodecylamine hydrochloride (cationic), potassium laurate (anionic), ethylbenzylammonium chloride (cationic), MP 635-S* (anionic), Antarox A-400† (nonionic), and protamine‡ (neutral ionic) solutions were used as emulsifying agents in some of the reactions. In other experiments, the monomer and organic starting material were either dissolved or suspended in the electrolyte.

In the few runs when polymerization occurred to the extent of 2–5 per cent, this formation was immediately evident. To ascertain the presence of polymer, in all runs methanol was added to the organic layer after each electrolysis. After those runs in which acetophenone was dissolved in the catholyte, distillation showed that there were no addition products, but only condensates from the ketone. The presence of monomer did not alter the amount, color, and melting point of the hexacarbothoxyethane. The amounts and color of the tarry material formed by the electrolyses of the quinolinium and diazonium salts with monomer in various ratios from 1:1 to 1:50 and without monomer were unchanged, and this was interpreted to mean that no addition products were formed in any runs.

The electrolyses of quinolinium and diazonium salts and of methyl iodide were carried out at smooth platinum electrodes. The procedure for the reduction of acetophenone has been described previously. Lead or platinum electrodes were used in all the anodic reactions.

One lead or lead oxide anode was a cylindrical sheet just fitting into a 400-ml tall type beaker. To make emulsification easier, another anode was made by plating lead on a ¼-in. wire mesh iron cylinder 4 in. high and 2 in. in diameter. The platinum cathode was a fine mesh cylinder 2 in. high and 1½ in. in diameter; it weighed 25 g. The platinum anode was a cylinder of similar mesh weighing 17 g; it was also 2 in. high and ½ in. in diameter.

Any discussion of this paper will appear in a Discussion Section, to be published in the June 1954 issue of the Journal.

* MP 635-S is an emulsifier compound of a 16 carbon sodium alkanesulfonate (49.5%), unreacted hydrocarbon (10.3%), sodium chloride (0.8%), sodium sulfate (0.4%), and isopropyl alcohol (3%) to maintain a homogeneous mixture. We are indebted to Dr. Stanley Detrich, Jackson Laboratory, E. I. du Pont de Nemours and Company, for this material.

† Antarox A-400 is a nonionic emulsifier prepared from the condensation of ethylene oxide with an alkylated phenol and was furnished to us by Mr. D. A. Beadell of General Aniline and Film Corporation.

‡ Protamine is a simple basic protein of low molecular weight furnished by Eli Lily and Company.

REFERENCES

1. E. Dineen, T. C. Schwan, and C. L. Wilson, *J. (and Trans.), Electrochem. Soc.*, **96**, 226 (1949).
2. I. M. Kolthoff and L. L. Ferstandig, *J. Polymer Sci.*, **6**, 563 (1951).
3. M. N. Das and S. R. Palit, *Science and Culture India*, **16**, 34 (1950).
4. R. G. R. Bacon, *Trans. Faraday Soc.*, **42**, 141 (1946).
5. S. Swann, Jr., and G. H. Nelson, *Trans. Electrochem. Soc.*, **67**, 201 (1935).
6. E. Gand, *Compt. rend.*, **226**, 1520 (1948).
7. B. Emmert, *Ber.*, **42**, 1997 (1909).
8. E. R. Atkinson, H. H. Warren, P. I. Abell, and R. E. Wing, *J. Am. Chem. Soc.*, **72**, 915 (1950).
9. G. Segré, Thesis, University of Illinois (1948).
10. K. Drees and G. Kowalski, *Brennstoff-Chem.*, **15**, 268 (1935).
11. S. Goldschmidt and E. Stöckl, *Chem. Ber.*, **85**, 630 (1952).
12. S. Swann, Jr., "Electrolytic Reactions," in "Technique of Organic Chemistry," Vol. II, (A. Weissberger, Editor), Interscience Publishers, Inc., New York (1948).

Structural Features of Oxide Coatings on Aluminum[1]

F. Keller, M. S. Hunter, and D. L. Robinson

Aluminum Research Laboratories, Aluminum Company of America, New Kensington, Pennsylvania

ABSTRACT

The structural features of the porous type of anodic oxide coating applied to aluminum have been investigated with the electron microscope. These coatings consist of close-packed cells of oxide, predominately hexagonal in shape, each of which contains a single pore. Pore size is a function of the electrolyte used and is independent of forming voltage. Wall thickness and barrier thickness are primarily a function of forming voltage and are affected to a minor degree by the electrolyte type. Pertinent dimensions of anodic coatings formed in sulfuric acid, oxalic acid, chromic acid, and phosphoric acid electrolytes are presented, and formulas are given for calculating the cell size and pore volume of these coatings.

Introduction

Anodic oxide coatings can be formed in various electrolytes under a wide variety of forming conditions, and, as a result, exhibit characteristics and behavior which are many and varied. Earlier work (1, 2) indicated the porous, cellular nature of certain of these coatings and developed fairly clear concepts of their manner of formation. This paper describes new and unique methods by which the intimate structural details of anodic oxide coatings can be revealed and by which the actual dimensions of the pores and oxide cells comprising these coatings can be determined. It also demonstrates the changes in dimensions effected by changes in electrolyte and forming voltage, and relates these microdimensions to the characteristics and behavior of the oxide coating.

Classification of Oxide Coatings

Anodic oxide coatings may be classified according to whether or not the electrolyte exerts appreciable solvent action on the oxide. In electrolytes that possess little or no ability to dissolve the oxide, the coatings are thin and nonporous, form rapidly, and have a thickness proportional only to the applied voltage. Coatings of this type, such as those formed in boric acid and borate electrolytes, possess unique electrical properties and have been used extensively in electrolytic capacitors and rectifiers.

With coatings formed in electrolytes that exert appreciable solvent action on the oxide, however, a relatively high, steady current flow and continued coating growth are observed. The amount of oxide formed is generally a function of current and time according to Faraday's law, although the final thickness of oxide obtained is naturally reduced by the solvent action of the electrolyte which is most pronounced at and near the outer surface of the oxide layer. Coatings of this type, such as those formed in sulfuric and chromic acid electrolytes, have been widely used for decorative purposes and in applications requiring resistance to wear and corrosion.

A specialized case of anodic coating formation in electrolytes that attack the oxide occurs with electrobrightening treatments. Here, the oxide is dissolved about as fast as it forms with the result that, at the end of the brightening treatment, only a very thin oxide film remains. This simultaneous formation and rapid solution of oxide tends to smooth out surface irregularities and thus produces a bright highly reflective surface.

The mechanism of formation is relatively simple for the first type, the "barrier" or "blocking" type of oxide coating. Initially, high current flows and oxide is formed rapidly but, after a relatively short time, current flow has decreased to a relatively low steady value and the coating is completely formed. Thickness is a function of applied voltage a t a rate of approximately 14 Å per volt and can be increased only by increasing the applied voltage (3). The low residual current represents, in part, "leakage" through constituent particles on which coating does not form and, as such, varies with the alloy and temper of the material under treatment.

In the second case, the process of coating formation is more complex. A barrier layer of oxide starts to form in the usual manner, but as soon as any oxide is formed, solvent action by the electrolyte also starts which tends to reduce the thickness of the barrier. From observation of the voltage and current excursions which occur at the start of

[1] Manuscript received January 9, 1953. This paper was prepared for delivery before the New York Meeting, April 12 to 16, 1953.

coating formation, these processes appear to reach a balance within a relatively short time, after which coating formation proceeds at a uniform rate.

Evolution of Oxide Cell Structure

Considering further the simultaneous solution and formation of oxide, it is possible to derive theoretically the basic structure of the porous type of oxide coating. This derivation is simplified by considering first the formation of a single cell of oxide by virtue of solvent action at a single point. When solvent action begins at this single point, the thickness of the oxide is reduced and current flows to repair the damage to the oxide layer. This raises the electrolyte temperature at this point and more rapid solution of oxide occurs. This mechanism would perpetuate a pore once it is formed, although other factors may halt the formation of some pores and start the formation of others.

As current continues to flow through the single pore under consideration and additional oxide forms, it is evident that an oxide cell must be created. Because the voltage and current fields about a point tend to be spherical, the advancing front of the oxide cell would be spherical if the pore was actually a point source. Since the pore is of finite size, however, the cell front will have the shape of a spherical section somewhat less than a hemisphere. The thickness of oxide between the metal and the pore base must be less than the value corresponding to 14 Å per volt because appreciable current is flowing. Also, the cell wall cannot be thicker because such thicknesses cannot form. Thus, as oxide is formed, a cylindrical cell, having a roughly hemispherical end and a central cylindrical pore, will be formed.

In actual practice, however, a continuous compact oxide layer rather than isolated ideal cells is formed. Consequently, the changes in shape necessary to form a compact layer must be considered. At the start of coating formation, the ideal cells probably do start to form, but if only cylindrical cells formed, intervening pillars of metal would remain. These pillars would still be in the effective electrical circuit and, therefore, would be converted to oxide. If consideration is given to the behavior that would be encountered if the oxide layer was composed of close packed cylinders, the final shape of the oxide cell is realized.

In such a close-packed array of cylinders, each cylinder would have line contact with six surrounding cylinders, and between each group of three contacting cylinders there would be a triangular pillar of metal with concave surfaces. As these pillars are converted to oxide anodically, the metal will be consumed equally from each face under the influence of the current from the pores of the three surrounding cells. When all the metal pillar is consumed in this fashion, the oxide layer will be continuous and the cells will have the form of hexagonal prisms rather than cylinders.

With this conversion of the ideal cylindrical cell to the actual close-packed array of hexagonal cells, changes in the shape of the pore also must occur. As the array changes from cylindrical to hexagonal shapes and the intervening metal is consumed, appreciable current will flow and localized heating and relatively rapid solvent action will result. Inasmuch as the metal to be consumed between

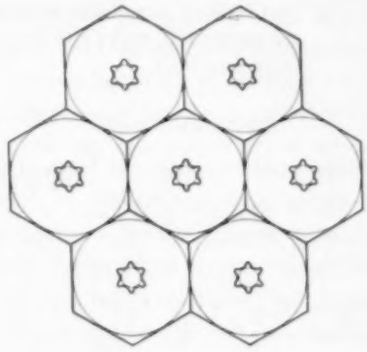

Fig. 1. Relation between ideal cylindrical oxide cells with cylindrical pores and close-packed hexagonal cells with star-shaped pores.

the cylindrical cells is not evenly distributed, current flow, heating, and solvent action will be localized, and the pore will be enlarged in proportion to the amount of metal consumed. Thus, the pore will no longer be cylindrical, but will have six projections, each directed toward a corner of the hexagon. The cross section of this shape should be roughly that of a six-pointed star, which will vary somewhat in shape according to the size of the pore. The relationship between the cylindrical structure and the hexagonal cell structure is shown in Fig. 1.

The change from isolated cylindrical cells to close-packed hexagonal cells also requires a change in the shape of the end of the oxide cell where it contacts the metal. Metal toward the junction of three adjoining cells will be under the influence of current from the pores in these cells and should be converted to oxide more rapidly by virtue of the higher current density resulting from the overlapping current fields. Consequently, the front of a single cell in a close-packed array will have a larger radius of curvature than that of a single isolated cell, and the cell front will have the shape of a spherical section somewhat less than a hemisphere.

On this basis, it can be predicted that an anodic oxide coating formed in an electrolyte that exhibits appreciable solvent action on the oxide is composed

of close-packed cells of oxide, each of which has the shape of a hexagonal prism. Each prism has a spherical shaped end and contains a centrally located pore, star-shaped in cross section. Through a combination of old and new methods of microscopic examination, it has now been proved that this is not merely the theoretical structure but is the actual structure of this type of anodic oxide coating.

Methods of Examination

In this investigation, the electron microscope was used almost exclusively because of the extreme fineness of the structures. In all, three different methods of approach were used. Cell base contours were determined through the use of polystyrene impressions and silica replicas (4) of cross sections of the oxide coatings. Considerable information regarding pore distribution and approximate pore size was gained by forming very thin anodic films and examining the oxide film itself by transmission in the electron microscope (2). When the oxide film is examined in this manner, the electron beam is blocked by the mass of the coating but passes through the pores and penetrates the thin oxide barrier at the pore bases. The pore structure is then seen on the viewing screen of the microscope as many fine, light dots, each of which corresponds to a pore in the coating.

The third method, and the one which was used most extensively, was extremely simple and is believed to be unique. This consisted of examining, through the use of aluminum oxide (5) and formvar replicas, the metal surface from which the oxide coating had been stripped. Inasmuch as the metal surface is in contact with the oxide coating at all times during coating formation, the cell base pattern in the metal reproduces in every detail the contour of the advancing oxide front. Thus, the dimensions of the metal surface are those of the oxide front.

In practice, the coating to be investigated was formed on a sample of high purity aluminum, the coating was stripped chemically, and either a plastic or aluminum oxide replica was made of the metal surface. The oxide was stripped by immersion in a hot (180°F) solution containing 35 cc of 85 per cent phosphoric acid and 20 grams of chromic acid per liter of solution. This dissolved the oxide coating but did not attack the metal. The aluminum oxide replicas were prepared by anodically coating the stripped aluminum sample at 17 volts in a 3 per cent tartaric acid solution adjusted to a *p*H of 5.5 with ammonium hydroxide. This produces a structureless replica about 240 Å thick, inasmuch as this tartrate solution is a "blocking" electrolyte.

Removal of the oxide replica from the metal is accomplished by amalgamation. The surface of the specimen is scribed to cut the replica into squares of a convenient size for handling, and the entire specimen is then immersed in concentrated mercuric chloride solution. When amalgamation has started,

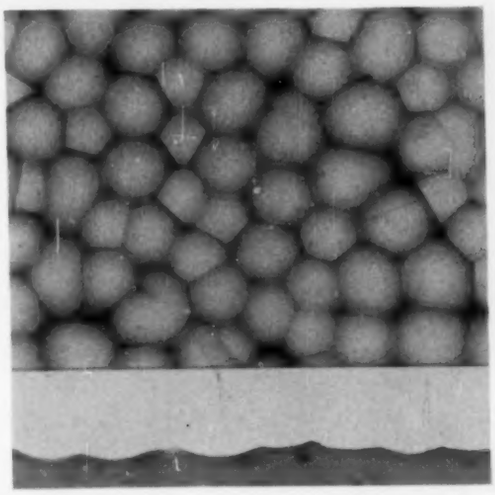

Fig. 2. Cell base pattern (top) of 120-volt phosphoric acid coating showing hexagonal cell structure and contour of cell base (bottom). Electron micrograph. Oxide film replica. 35,000×.

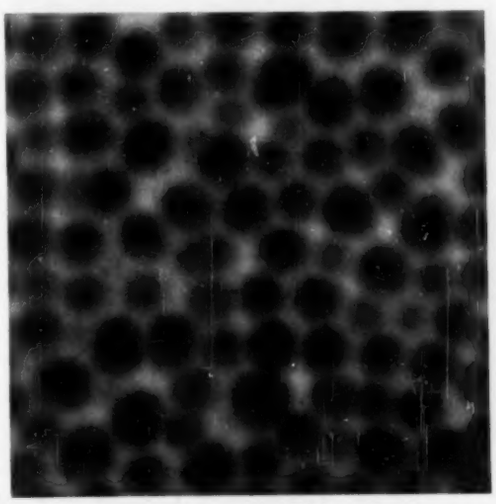

Fig. 3. Cell base pattern of 120-volt phosphoric acid coating showing hexagonal cells and peaks and ridges between cells. Electron micrograph. Formvar replica. 35,000×.

as indicated by deposition of mercury along the scribed lines, the specimen is transferred to distilled water and amalgamation is allowed to continue until the squares of oxide separate from the metal. These squares are transferred to a distilled water wash, then picked up on the electron microscope screens, and allowed to dry.

Oxide Structures

Coatings formed in sulfuric acid, chromic acid, phosphoric acid, and oxalic acid electrolytes were

examined as described above. The basic structure of the coatings formed in all of these electrolytes was the same, and proved that the structure of the coatings derived theoretically is correct. Coatings formed in a 4 per cent phosphoric acid electrolyte are

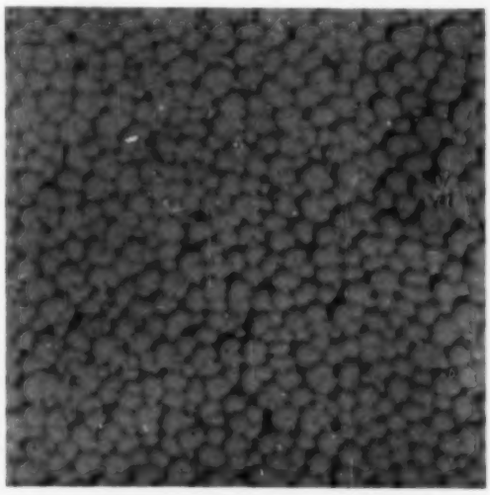

FIG. 4. Cell base structure of 30-volt phosphoric acid coating. Electron micrograph. Oxide film replica. 35,000×.

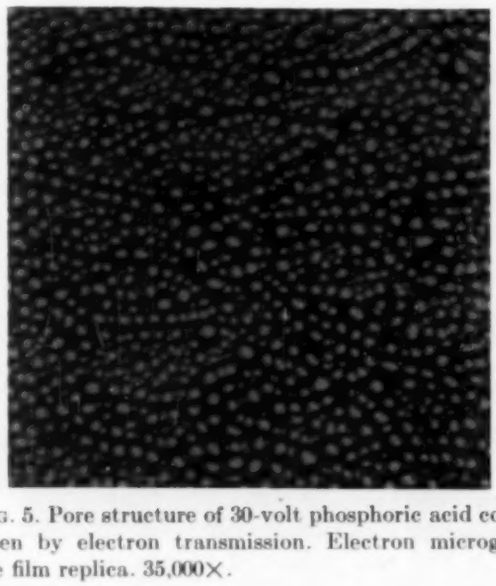

FIG. 5. Pore structure of 30-volt phosphoric acid coating as seen by electron transmission. Electron micrograph. Oxide film replica. 35,000×.

used to demonstrate the cell and pore structure and the manner in which the dimensions of the porous type of oxide coating can be determined.

The predominately hexagonal shape of the cells of oxide in this type of coating is shown very clearly by the cell base pattern of a coating formed at 120 volts in the 4 per cent phosphoric acid electrolyte (Fig. 2). In a formvar replica (6) of the same surface, the hexagonal cell shape is again visible and, in addition, the minute ridges and peaks between cells are apparent (Fig. 3). In this type of replica, depressions are filled by the formvar, whereas high points retain only a thin coating of plastic. Consequently, the cups representing the ends of the cells appear dark and the peaks and ridges between cells appear lighter in shade. The contour of the end of the oxide cells is seen in a replica of a cross section of this same sample (Fig. 2). The scalloped appearance of this section shows clearly that the ends of the cells represent a spherical section less than a hemisphere. All the scallops are not of equal size because this particular section did not run directly across the centers of the cups.

Examinations of the pore structure by electron transmission could not be carried out with the

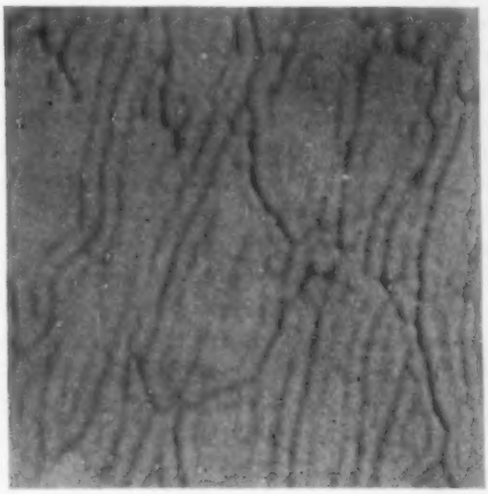

FIG. 6. Cell base pattern of 40-volt phosphoric acid coating at 1½ min showing start of cell formation along subgrain boundaries. Electron micrograph. Oxide film replica. 35,000×.

120-volt phosphoric acid coating, because the barrier at the pore bases was too thick to be penetrated by the electron beam. The relation between cell structure and pore structure is evident, however, by comparison of the cell base pattern (Fig. 4) and the pore pattern (Fig. 5) of a coating formed in the same phosphoric acid electrolyte at 30 volts. From these electron micrographs, it is apparent that there are as many pores as cells and that the cell size and pore spacing are the same.

It has not yet been possible to see the star-shaped contour of the pores, because the difference in size between the star and the ideal cylindrical pore would be only about 45 Å even with the largest pores examined.

Following this same line of approach, some interesting and unique facts are revealed regarding the method of formation, dimensions, and behavior of the porous type of anodic oxide coating. Of considerable interest is the manner in which this type of coating starts to form. Initially, single rows of cells form along either side of the subgrain boundaries of the aluminum as shown by Fig. 6. Forma-

tion starts in these regions because the natural oxide film at such boundaries is not as compact or continuous and offers less resistance to current flow. As the coating process continues, additional rows of cells are formed within the subgrains (Fig. 7) until, finally, a well developed cell pattern is apparent and the identity of the subgrain structure has been masked (Fig. 4). Once the cell pattern has been well established, further formation does not alter the pattern unless forming conditions are changed.

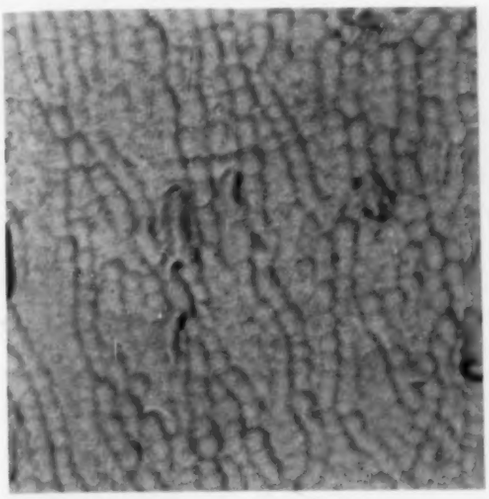

FIG. 7. Cell base pattern of 40-volt phosphoric acid coating after 2 min showing formation of additional cells within subgrains. Electron micrograph. Oxide film replica. 35,000×.

OXIDE CELL DIMENSIONS

Interesting information is gained by following the changes that occur in the cell base pattern with changes in formation voltage. As might be expected, the oxide cell size increases with voltage (Fig. 8) and, if cell size is plotted against forming voltage, it is apparent that this increase is linear (Fig. 9). Thus, cell size is a direct function of voltage as it is in the case of coatings formed in electrolytes that do not dissolve the oxide. In the present case, however, the straight-line plot does not go through the origin so that cell size must also be a function of some other factor.

The structure of the individual oxide cells reveals the variables that affect cell size, and permits actual determination of the cell dimensions. Basically, each cell is composed of a pore, an oxide wall, and a barrier oxide layer at its base. The over-all cell size can be measured directly from micrographs of the cell base pattern. This cell is not solid oxide, however, and has a diameter equal to twice the thickness of the oxide wall plus the diameter of the pore.

With this in mind, it is evident that the straight-line plot seen in Fig. 9 can be obtained in either of two ways. Such a plot would result if the oxide wall did not increase linearly with voltage, and any departure from linearity was offset by an equal and opposite change in pore diameter. Such a balance

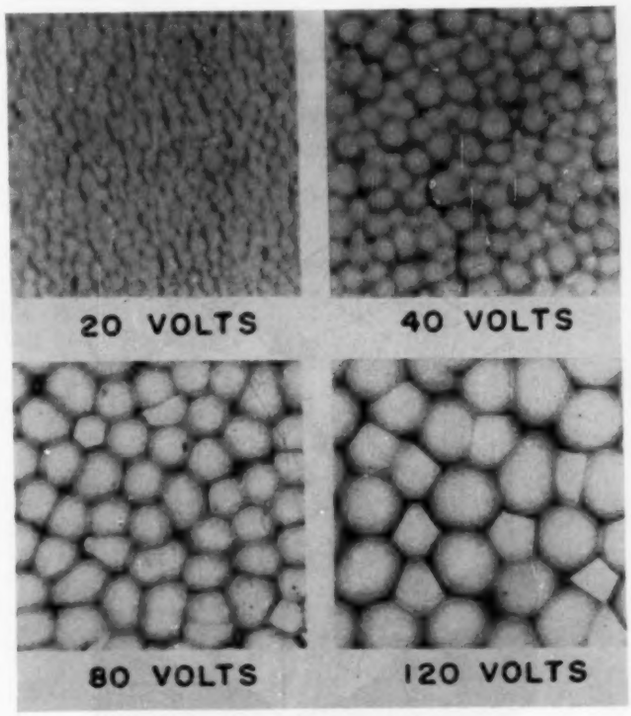

FIG. 8. Cell base patterns of coatings formed in 4% phosphoric acid electrolyte showing increase in oxide cell size with forming voltage. Electron micrograph. Oxide film replicas. 35,000×.

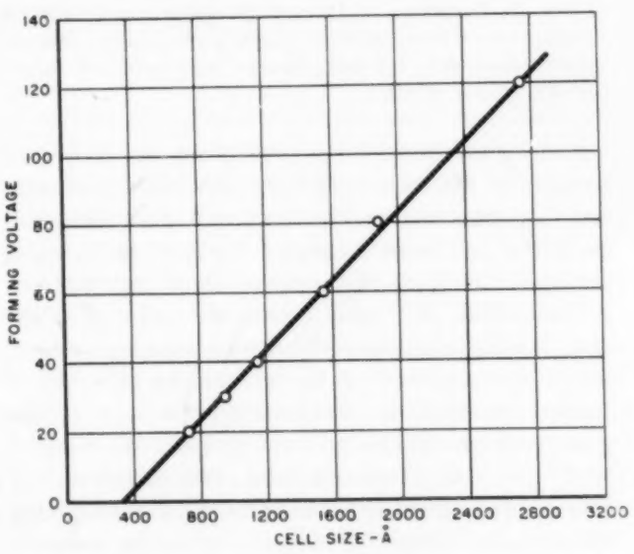

FIG. 9. Relation between cell size and forming voltage in 4% phosphoric acid electrolyte.

does not appear reasonable. The more likely reason for the straight-line plot is that the thickness of the oxide wall does increase linearly with voltage, and the pore diameter remains constant. On this basis, the difference between the cell size and the

thickness of oxide comprising the two sides of the cell wall should be a constant value, the pore diameter. This value is obviously the amount by which the plot of cell size against voltage is transposed from the origin. Accordingly, pore size is represented by the point at which the straight line intersects the size axis. Thus, in the case of the coating formed in the 4 per cent phosphoric acid electrolyte, the pore diameter is found to be about 330 Å.

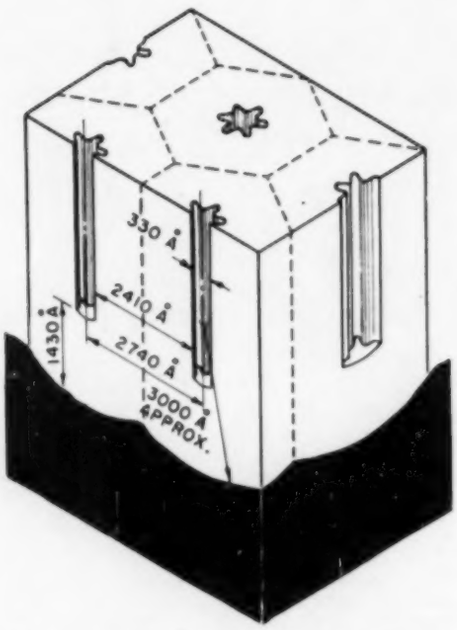

FIG. 10. Structure of 120-volt phosphoric acid coating constructed on cross section of cell base pattern. Dimensions of pore, cell, cell wall, barrier, and radius of curvature are shown. 65,000×.

Having established the pore diameter, it is now possible to determine other dimensions of the oxide cell. By subtracting the constant pore diameter from the cell sizes measured for various forming voltages, the total thickness of oxide wall per cell is found. Half this value is then the cell wall thickness. If wall thickness is divided by forming voltage, the thickness of oxide in the cell wall for each volt of applied potential is obtained. In the case of the 4 per cent phosphoric acid electrolyte, this value is 10.0 Å per volt. From this value, the cell size at any forming voltage may be calculated by multiplying the forming voltage by 10.0, doubling this value to take into account the oxide thickness at both sides of the cell, and adding the 330 Å pore diameter. From these relationships between cell size, forming voltage, and pore size, a scale model of the oxide cell array formed in this electrolyte may be constructed. Such a scale model of the 120-volt phosphoric acid coating is shown in Fig. 10 with the corresponding cross section of the cell base pattern.

Referring to the contour of the cell base pattern, which consists of spherical sections less than a hemisphere, it is possible to determine the radius of curvature and the location of the center of curvature of the cell and pore bases. These can be found by measuring the height and width of the pore base cross sections and applying the formula

$$R = H/2 + W^2/8H$$

where R is the radius of curvature, H is the height of the scallop, and W is the width of the scallop (cell size). In the case of the 120-volt phosphoric acid coating, the radius of curvature is found to be about 3000 Å, which places the center of curvature well up inside the pore at the point indicated in Fig. 10. This point apparently represents the hypothetical current distribution point for the pore.

Cell and pore dimensions of coatings formed in 2 per cent oxalic acid, 3 per cent chromic acid, and 15 per cent sulfuric acid electrolytes were also determined. The oxalic acid electrolyte was operated at 75°F and the chromic acid electrolyte at 100°F. The sulfuric acid electrolyte had to be cooled to 50°F to obtain some of the voltages desired.

The relationships between cell size, pore size, and forming voltage in these electrolytes were the same as those observed in the phosphoric acid electrolyte. As would be expected, however, cell size and pore diameter were appreciably different with the several electrolytes. In these electrolytes, pore diameter apparently is determined by the electrolyte and is not affected by forming voltage. Wall thickness is controlled primarily by forming voltage, but is also related to the particular electrolyte by virtue of the different thickness of oxide formed per volt of applied potential. Inasmuch as cell size is equal to the sum of the pore diameter and twice the wall thickness, cell size is determined by both the electrolyte and the voltage employed to form the coating.

The cell and pore structures of coatings formed at several voltages in one of the electrolytes investigated are shown by Fig. 11 and the relation between cell size and forming voltage in the four electrolytes is shown graphically by Fig. 12. The pore diameters and wall thickness values in these same electrolytes are given in Table I. These pore dimensions apply only to pore diameter at the base of the pores and do not take into account any possible widening of the pores resulting from solvent action along the pore walls. Also, the values given apply only to the particular electrolyte concentrations and temperatures, although additional work indicates that changes in concentration and temperature of an

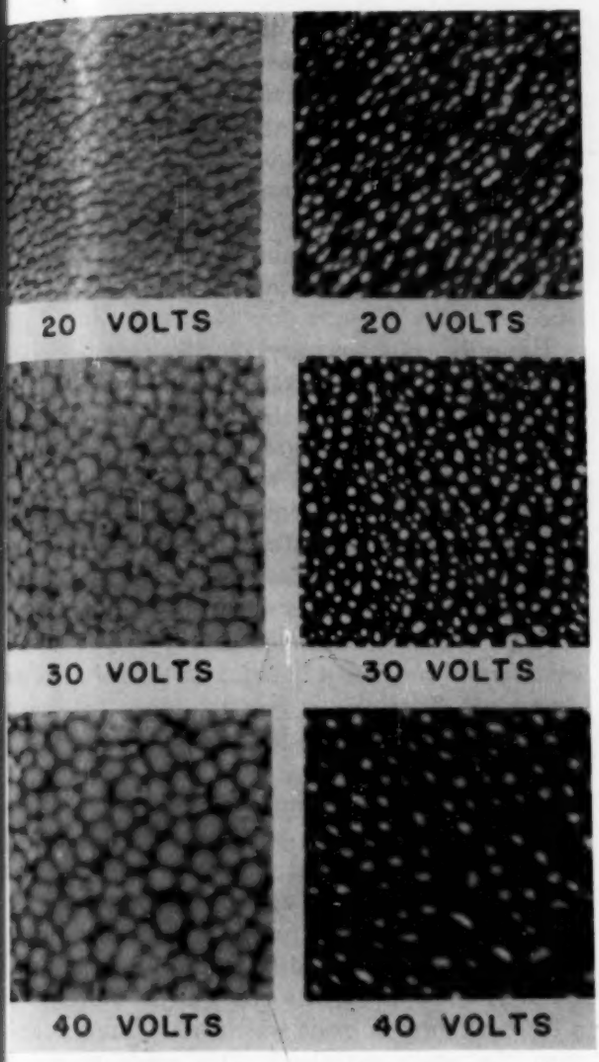

FIG. 11. Cell (left) and pore (right) structures of coatings formed in 4% phosphoric acid electrolyte. Electron micrograph. Oxide film replicas. 35,000×.

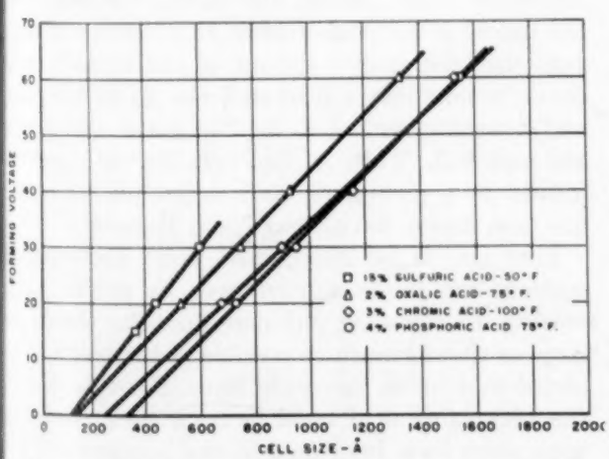

FIG. 12. Relation between cell size and forming voltage in anodic coating electrolytes.

electrolyte may have only a small effect on the pore and cell size.

The cell size of coatings formed at any voltage in these electrolytes can be calculated from the equation

$$C = 2WE + P$$

where C is cell size, W is wall thickness in Å per volt, E is forming voltage, and P is pore diameter.

TABLE I. *Pore diameter and wall thickness values of oxide coating*

Electrolyte	Pore diameter, Å	Wall thickness Å per volt
4% Phosphoric acid, 75°F	330	10.0
2% Oxalic acid, 75°F	170	9.7
3% Chromic acid, 100°F	240	10.9
15% Sulfuric acid, 50°F	120	8.0

TABLE II. *Number of cells or pores in oxide coatings*

Electrolyte	Volts	No. per in.^{2} × 10^9
15% Sulfuric acid, 50°F	15	498
15% Sulfuric acid, 50°F	20	334
15% Sulfuric acid, 50°F	30	179
2% Oxalic acid, 75°F	20	230
2% Oxalic acid, 75°F	40	75
2% Oxalic acid, 75°F	60	37
3% Chromic acid, 120°F	20	140
3% Chromic acid, 120°F	40	52
3% Chromic acid, 120°F	60	27
4% Phosphoric acid, 75°F	20	121
4% Phosphoric acid, 75°F	40	50
4% Phosphoric acid, 75°F	60	27

An interesting feature of the wall thickness data for the various electrolytes is that another investigation, as yet unpublished, has shown that the barrier oxide thicknesses at the oxide cell bases are in the same order in these four electrolytes. The actual thickness of the barrier at the cell bases, however, appears to be greater by a factor of 1.1 to 1.2.

The actual number of cells in anodic oxide coatings can best be appreciated by translating the cell size values to its reciprocal cell numbers, in visible dimensions. The number of cells and, consequently, the number of pores runs into hundreds of thousands per inch and into billions per square inch. The numbers of cells for coatings formed in the four electrolytes investigated are given in Table II.

With values of pore number and diameter available, calculations of pore volume can be made. Pore volume must decrease with increasing formation voltage because cell size is increasing, the number of cells per unit area is decreasing, and the pore diameter remains constant. Assuming that the pores are circular in section, a close approximation

to the star shape as discussed earlier, the pore volume of a coating may be calculated from the equation

$$V = 78.5\ P^2/C^2$$

where V is pore volume in per cent, P is pore diameter, and C is cell size. The relationship between pore volume and forming voltage in the electrolytes investigated is shown by Fig. 13. In actual practice, pore volume is generally greater than these calculated values because of solvent action occurring

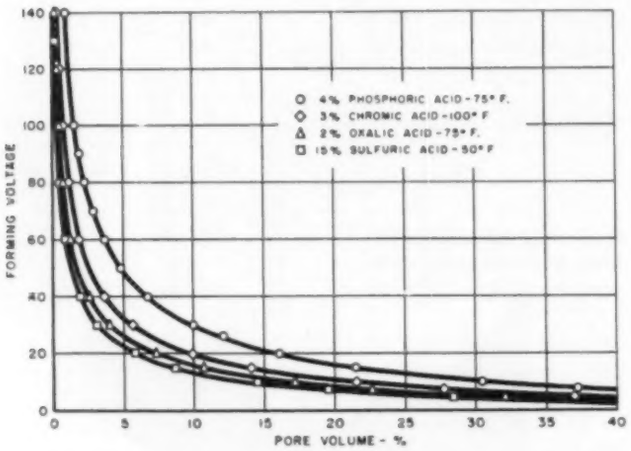

FIG. 13. Relation between pore volume and forming voltage in anodic coating electrolytes.

along pore walls and at the surface of the coating during the time of formation.

Consideration has thus far been given to anodic coating formation where the final oxide layer is the desired end product. Electrobrightening is actually a similar type of anodic coating treatment but, in this case, a final oxide layer is undesirable. Accordingly, the ideal electrobrightening treatment would be one in which the oxide layer was dissolved as fast as it was formed. In commercial treatments, however, this is not practical, and electrobrightened articles have a thin oxide film or "smudge" which must be removed to obtain maximum brightness.

Examinations of electrobrightened surfaces in the manner described prove that this type of treatment actually involves the formation of a porous type of oxide coating. Surfaces brightened by a treatment that operates at 15 volts in a fluoboric acid electrolyte[2] and by one that is carried out at 20 volts in a phosphoric acid-carbitol electrolyte were examined. In each case, the cell base pattern characteristic of the porous type of oxide coating was apparent.

[2] Patented process licensed by Aluminum Company of America.

SIGNIFICANCE OF OXIDE CELL DIMENSIONS

The various structures and dimensions of the porous type of anodic oxide coating described are of considerable interest from the theoretical viewpoint. Of even greater importance is the fact that they explain many of the aspects of anodic coating behavior and may be used to formulate combinations of electrolytes and forming conditions to produce anodic oxide coatings having certain specific desirable characteristics.

Basically, the behavior of this type of anodic coating is a function of four variables: namely, pore size, cell wall thickness, the barrier thickness at the base of the pore, and the character of the oxide formed. Investigation of this latter variable is not within the scope of this paper. Of the dimensional variables, wall thickness and barrier thickness are primarily a function of the forming voltage and cannot be greater than 14 Å times the applied voltage. In all cases investigated, they were less by a factor that was a function of the nature of the electrolyte. Pore size is found to be a function of the electrolyte and is independent of forming voltage.

With these facts in mind, consideration may be given to the relation between electrolytes and forming conditions and the characteristics and performance of the coating. In sealing anodic oxide coatings, pore size is of primary importance. When oxide coatings are sealed in boiling water, some of the oxide comprising the cell wall is converted to a different form of oxide which has a larger volume than the oxide consumed. This tends to seal or plug the pores and prevent access of substances into the coating or to the underlying metal. In sealing an oxide coating, the smaller the pore size, the tighter is the plug created. In a coating of large pore size, the greater volume of the oxide formed during sealing may not be sufficient to fill the pore, and complete sealing in boiling water cannot be accomplished. This is the behavior of coatings formed in a phosphoric acid electrolyte which, as has been shown, have a large pore diameter.

Pore size is of importance when electroplated coatings are to be applied over an anodic oxide coating. In this case, the pore diameter should be large so that as much as possible of the metal to be plated may enter the oxide layer. For this reason, the phosphoric acid coatings with their relatively large pores have been used in this application.

In the matter of hardness and resistance to wear and abrasion, pore volume or, conversely, the amount of massive oxide is of prime importance. Inasmuch as the massive oxide is the material that supports the load and resists the wear, increases in

hardness and wear resistance can be obtained by decreasing the size and number of the pores. This can be done by choosing an electrolyte that develops small pores and by using high forming voltage to increase cell size and cell wall thickness and thereby decrease the number of cells and pores in a given area.

For resistance to corrosion, pore and cell size and, particularly, thickness of the oxide barrier at the pore bases are important. When an oxide coating is used to protect aluminum from corrosion, its primary function is to prevent the corroding medium from coming in contact with the metal. The easiest approach is through the pores and then through the barrier layer at the pore base. Thus, decreasing the pore size by choosing an electrolyte that characteristically develops small pores makes access to the pore base more difficult. Also, if the thickness of barrier is increased by increasing the forming voltage, more time is required for the corroding medium to dissolve through this portion of the coating and come in contact with the metal.

These examples are but a few of the many ways in which this method of approach may be used to solve anodic oxide coating problems. It can be used to establish the dimensions of the fundamental oxide cell formed in any electrolyte and under any combination of forming conditions. With a knowledge of these dimensions and their relation to behavior, it is then possible to produce coatings specifically designed for particular applications.

Any discussion of this paper will appear in a Discussion Section, to be published in the June 1954 issue of the JOURNAL.

REFERENCES

1. J. D. EDWARDS AND F. KELLER, *Trans. Electrochem. Soc.*, **79,** 135 (1941).
2. J. D. EDWARDS AND F. KELLER, *Trans. Am. Inst. Mining Met. Engrs.*, **156,** 288 (1944).
3. G. HASS, *J. Opt. Soc.*, **39,** 532 (1949).
4. R. D. HEIDENREICH AND V. G. PECK, *J. Appl. Phys.*, **14,** 23 (1943).
5. F. KELLER AND A. H. GEISLER, *Trans. Am. Inst. Mining Met. Engrs.*, **156,** 82 (1944).
6. V. J. SCHAFER AND D. HARKER, *J. Appl. Phys.*, **13,** 427 (1942).

Sustaining Members of The Electrochemical Society

Air Reduction Company, Inc., New York, N. Y.

Ajax Electro Metallurgical Corporation, Philadelphia, Pa.

Alloy Steel Products Company, Inc., Linden, N. J.

Aluminum Company of America, New Kensington, Pa.

Aluminum Company of Canada, Ltd., Montreal, Canada

American Machine & Foundry Co., Raleigh, N. C.

American Platinum Works, Newark, N. J. (2 memberships)

American Potash & Chemical Corp., Los Angeles, Calif.

American Zinc, Lead and Smelting Company, St. Louis, Mo.

Armour Research Foundation, Chicago, Ill.

Auto City Plating Company Foundation, Detroit, Mich.

Bell Telephone Laboratories, Inc., New York, N. Y.

Bethlehem Steel Company, Bethlehem, Pa. (2 memberships)

Buffalo Electro-Chemical Company, Buffalo, N. Y.

Burgess Battery Company, Freeport, Ill.

Canadian Industries Limited, Montreal, Canada

Chrysler Corporation, Detroit, Mich.

Columbia-Southern Chemical Corporation, Pittsburgh, Pa.

Consolidated Mining and Smelting Company of Canada, Ltd., Trail, B. C. (2 memberships)

Corning Glass Works, Corning, N. Y.

Crane Company, Chicago, Ill.

Diamond Alkali Company, Pittsburgh, Pa. (2 memberships)

Dow Chemical Company, Midland, Mich.

Wilbur B. Driver Co., Newark, N. J.

E. I. du Pont de Nemours & Company, Inc., Wilmington, Del.

E. I. du Pont de Nemours & Company, Screen Division, Towanda, Pa.

Eagle-Picher Company, Joplin, Mo.

Eaton Manufacturing Company, Stamping Div., Cleveland, Ohio

Electric Auto-Lite Company, Toledo, Ohio

Electric Storage Battery Company, Philadelphia, Pa.

The Eppley Laboratory, Newport, R. I.

Ford Motor Company, Dearborn, Mich.

General Chemical Division, Allied Chemical & Dye Corporation, New York, N. Y.

General Electric Company, Schenectady, N. Y.

General Motors Corp., Research Laboratories Division, Detroit, Mich.

Gould-National Batteries, Inc., Depew, N. Y.

Graham, Crowley & Associates, Inc., Chicago, Ill.

Great Lakes Carbon Corporation, Niagara Falls, N. Y.

Hanson-Van Winkle-Munning Company, Matawan, N. J. (2 memberships)

Harshaw Chemical Company, Cleveland, Ohio (2 memberships)

Hooker Electrochemical Company, Niagara Falls, N. Y. (3 memberships)

Houdaille-Hershey Corporation, Detroit, Mich.

International Graphite & Electrode Div., Speer Carbon Co., St. Marys, Pa. (2 memberships)

International Minerals & Chemical Corporation, Chicago, Ill.

International Nickel Company, Inc., New York, N. Y. (3 memberships)

Kaiser Aluminum & Chemical Corp., Division of Metallurgical Research, Spokane, Wash.

Mathieson Chemical Corporation, Niagara Falls, N. Y.

McGean Chemical Company, Cleveland, Ohio

Merck & Company, Inc., Rahway, N. J.

Metal & Thermit Corporation, New York, N. Y.

Monsanto Chemical Company, St. Louis, Mo.

National Carbon Division, Union Carbide and Carbon Corporation, New York, N. Y. (2 memberships)

National Cash Register Company, Dayton, Ohio

National Research Corporation, Cambridge, Mass.

Niagara Alkali Company, Niagara Falls, N. Y.

Norton Company, Worcester, Mass.

Pennsylvania Salt Manufacturing Company, Philadelphia, Pa.

Philco Corporation Co., Lansdale, Pa.

Philips Laboratories, Inc., Irvington-on-Hudson, N. Y.

Potash Company of America, Carlsbad, N. Mex.

Promat Division, Poor & Company, Waukegan, Ill.

Ray-O-Vac Company, Madison, Wis.

Sarkes Tarzian, Inc., Bloomington, Ind.

Solvay Process Division, Allied Chemical & Dye Corporation, Syracuse, N. Y. (3 memberships)

Stackpole Carbon Company, St. Marys, Pa.

Standard Steel Spring Company, Coraopolis, Pa.

Stauffer Chemical Company, San Francisco, Calif.

Sylvania Electric Products Inc., Bayside, N. Y. (2 memberships)

Tennessee Products & Chemical Corporation, Nashville, Tenn.

Udylite Corporation, Detroit, Mich. (2 memberships)

Union Carbide Company, Electrometallurgical Division, New York, N. Y.

United Chromium, Inc., New York, N. Y.

Vanadium Corporation of America, New York, N. Y.

Victor Chemical Works, Mt. Pleasant, Tenn.

Wagner Brothers, Inc., Detroit, Mich.

Western Electric Company, Inc., Chicago, Ill.

Western Electrochemical Company, Los Angeles, Calif.

Westinghouse Electric Corporation, E. Pittsburgh, Pa.

Willard Storage Battery Company, Cleveland, Ohio.

Yardney Electric Corp., New York, N. Y.